Chapter 3

Signal Model and System Definitions

A general system description and signal model definitions are needed before designing linearization algorithms. Many of the definitions and notations included in this chapter will be referenced later and will be applied to the formulation of the algorithms. Theoretical analysis and characterization of the signal model is developed in order to support the subsequent signal processing strategies. The importance and advantages of choosing OFDM as the modulation scheme for the signal model will become more evident as the model structure is developed within these sections.

3.1 General System Description

The general definitions regarding the generation and structure of the OFDM signal will be of great interest in order to design the digital processing strategies for linearization presented in this work. Therefore, a first revision of the OFDM basics can be helpful to establish some properties that could be exploited in later chapters.

The general principles of the OFDM system have been analyzed and described in very few comprehensive technical literature such as [8]. The numerous theoretical aspects that a complete characterization of OFDM would imply, have not been unified yet in a single reference, being instead inherent to a wide range of specific documents. Besides this, in the past few years an increasing number of researchers have devoted their efforts to mainly providing performance assessments of OFDM-based systems reported in various technical publications. Moreover, the inner details of the OFDM signal structure normally appear as specific contents in a variety of technical standards available for last-generation digital communication systems [2][3][4]. However, there exists a relative shortage of theoretical publications on some aspects of OFDM theory. Many issues within this field still deserve further treatment. For instance, the impact of the interaction between the D/A domains in presence of a highly non-linear channel constitutes an interesting research topic whose detailed study could help assessing the

higher-level models in which some linearization strategies are based on. In light of this, it is worthwhile to review the basic formulation of the OFDM signal model in order to gain insight for the development of a more detailed discussion of the OFDM signal model, focusing specifically on the treatment of the non-linearity problem. Thus, along this section we shall point out some crucial formulations in order to make the thesis self-contained in terms of the particular signal model that will apply henceforth.

3.1.1 OFDM Signal Generation

Basically, the OFDM signal is made up of a sum of N complex orthogonal subcarriers (indexed with $k = \{0, 1, 2, \ldots, N-1\}$), each one independently modulated by using M-QAM data d_k. If we let f_c be the RF carrier frequency, then one OFDM symbol with duration T and starting at $t = t_s$ has the following passband expression in the time domain:

$$s(t) = \begin{cases} \mathrm{Re}\left\{ \sum_{k=0}^{N-1} d_k e^{j2\pi\left(f_c + \frac{(N-1-2k)}{2T}(t-t_s)\right)} \right\} & ; \quad t \in [t_s, t_s + T] \\ 0 & ; \quad otherwise. \end{cases} \tag{3.1}$$

Nevertheless, as demonstrated in later sections, the distortion effect introduced by RF non-linear amplifiers in a complex passband signal like (3.1), can be completely characterized in base-band which is computationally more efficient. Therefore, we will often concentrate our analysis on the base-band equivalent model (also called low-pass equivalent) of the OFDM signal and its corresponding communication system representation.

Figure 3.1 shows a representation of a general OFDM system, where the modulation and demodulation are performed as block-oriented processes that can be efficiently implemented through the Fast Fourier Transform (FFT) algorithm. In this system, the incoming M-QAM symbols are critically sampled (one sample per information symbol/subcarrier) and grouped within the column vector $\mathbf{d}_x = \Big[d_x[0] \cdots d_x[N-1] \Big]^T$, thus forming the information signal blocks of length N. The symbols $d_x[n]$ are generated at a rate $f_s = 1/T_d$, and modulate separately the N orthogonal subcarriers during the whole i-th time interval $\mathcal{I}_i = [iT, iT + T]$, defined for one OFDM symbol with period $T = NT_d = N/f_s$. Then, the continuous time complex envelope of the base-band OFDM signal can be written for any instant t as

$$b_x(t) = \frac{1}{\sqrt{N}} \sum_{k=0}^{N-1} d_x(k, i) e^{j2\pi f_k t}, \quad \text{for } t \in \mathcal{I}_i \tag{3.2}$$

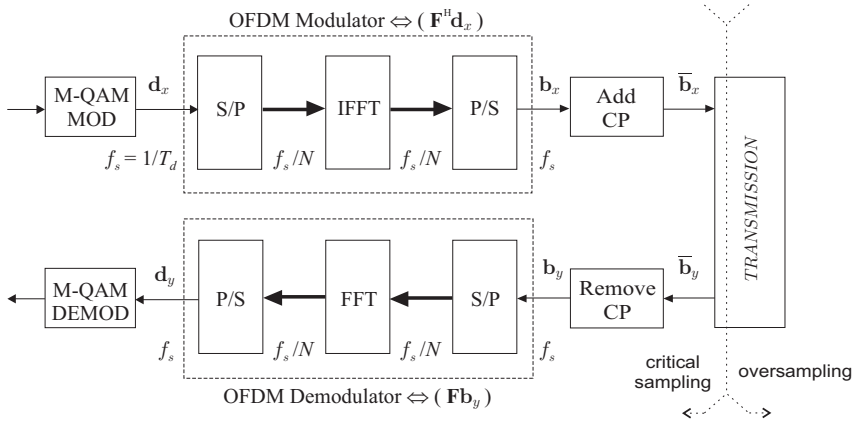

Figure 3.1: Block diagram of the OFDM modulation stages.

where $f_k = \frac{k\,f_s}{N} = \frac{k}{T}$ is the k-th subcarrier frequency, and $d_x(k,i)$ is the M-QAM symbol modulating the k-th carrier during the whole i-th OFDM symbol interval. As a definition of stationarity for OFDM signals, $d_x(k,i)$ are normally assumed to be mutually independent and identically distributed symbols from an M-QAM alphabet $\mathcal{M} = \left[(2m-1-\sqrt{M}) + j(2n-1-\sqrt{M})\right]; (m,n) = \{1,2,\ldots,\sqrt{M}\}$. According to this, and unless otherwise indicated in specific sections, we will constrain our analysis (without loss of generality) to the first OFDM symbol, transmitted in the interval $\mathcal{I}_0$. Then, from (3.2) the corresponding OFDM symbol at the critical sampling rate f_s, consists of the set of T_d-spaced base-band signal samples $\mathbf{b}_x = \left[b_x[0]\cdots b_x[N-1]\right]^T$ (elements $b_x[n] = b_x(nT_d)$, with $n = \{0,\ldots,N-1\}$) obtained by taking the IDFT of the first incoming data frame $\mathbf{d}_x$ (elements $d_x(k,0) = d_x[k]$, with $k = \{0,1,\ldots,N-1\}$). The n-th element in the discrete-time base-band signal vector $\mathbf{b}_x$ is then given by

$$b_x[n] = b_x(nT_d) = \frac{1}{\sqrt{N}} \sum_{k=0}^{N-1} d_x[k] e^{j\frac{2\pi}{N}nk} w\left[n/(N-1)\right] \tag{3.3}$$

where $w[\cdot]$ is a discrete rectangular window that is defined by

$$w[r] = \begin{cases} 1 & ; \quad 0 \le r \le 1 \\ 0 & ; \quad \text{otherwise.} \end{cases} \tag{3.4}$$

Then, for the one step generation of $\mathbf{b}_x$, the calculation of (3.3) for $(n,k) = \{0,\ldots,N-1\}$, can be equivalently performed as the following matrix operation:

$$\mathbf{b}_x = \mathbf{F}^{\mathrm{H}}\mathbf{d}_x \tag{3.5}$$

where $\mathbf{F}$ is the DFT matrix whose hermitian is associated to the inverse operation IDFT. According to (3.3) and (3.5) this DFT matrix can be defined as

$$\mathbf{F}_{(N\times N)} = \frac{1}{\sqrt{N}} \begin{bmatrix} 1 & 1 & 1 & 1 & \cdots & 1 \\ 1 & e^{-j\frac{2\pi}{N}} & e^{-j\frac{4\pi}{N}} & e^{-j\frac{6\pi}{N}} & \cdots & e^{-j2\pi\frac{N-1}{N}} \\ 1 & e^{-j\frac{4\pi}{N}} & e^{-j\frac{8\pi}{N}} & e^{-j\frac{12\pi}{N}} & \cdots & e^{-j4\pi\frac{N-1}{N}} \\ 1 & e^{-j\frac{6\pi}{N}} & e^{-j\frac{12\pi}{N}} & e^{-j\frac{18\pi}{N}} & \cdots & e^{-j6\pi\frac{N-1}{N}} \\ \vdots & \vdots & \vdots & \vdots & \ddots & \vdots \\ 1 & e^{-j2\pi\frac{N-1}{N}} & e^{-j4\pi\frac{N-1}{N}} & e^{-j6\pi\frac{N-1}{N}} & \cdots & e^{-j2\pi\frac{(N-1)^2}{N}} \end{bmatrix} \tag{3.6}$$

where we can easily observe the important condition:

$$\mathbf{F}^{\mathrm{H}}\mathbf{F} = \mathbf{I}_{(N)}. \tag{3.7}$$

Note that every column in (3.6) corresponds to a complex subcarrier with a normalized frequency that depends on the size of the FT (N must be power of 2 in order to perform IFFT and FFT using a radix-2 or radix-4 algorithm [8]).

To simplify the basic signal model description we assume for the moment that the transmission block shown in figure 3.1 is characterized by a perfectly linear discrete transfer function. Thus, the different transmission stages therein embedded (such as D/A-A/D converters, filters and the non-linear HPA) shall be subsequently added and its effects discussed in later sections to complete the real system description. Then, according to the previous assumption, in reception, the FFT is applied to the transmitted base-band signal samples $b_y[m]$ to recover the original M-QAM data. Hence, the k-th data symbol given to the M-QAM demodulator is obtained as follows:

$$d_y[k] = \frac{1}{\sqrt{N}} \sum_{m=0}^{N-1} b_y[m] e^{-j\frac{2\pi}{N}mk}. \tag{3.8}$$

The vector $\mathbf{d}_y = \Big[d_y[0] \cdots d_y[N-1]\Big]^T$, with the demodulated M-QAM symbols from the respective transmitted block, can also be obtained as the FFT of the received sequence $\mathbf{b}_y$:

$$\mathbf{d}_y = \mathbf{F}\mathbf{b}_y. \tag{3.9}$$

Along with (3.1) through (3.9), we could also refer to OFDM signals in a more general form with a pair of passband and base-band equivalent signal models in the form,

$$s_p(t) = Re\left\{b_x(t)e^{j2\pi f_c t}\right\} \tag{3.10}$$

$$b_x(t) = u_x(t)e^{j\alpha_x(t)} \tag{3.11}$$

respectively, where $u_x(t) = |b_x(t)|$ corresponds to the complex envelope of the base-band signal. If we let (3.11) be a simplified representation of the OFDM signal in (3.2) we have that, for large values of N (> 100) and by means of the Central Limit Theorem, the CDF of $b_x(t)$ can be well approximated by that of a zero-mean complex Gaussian random process with uncorrelated in-phase and in-quadrature components. Thus, the modulus $u_x(t) = |b_x(t)|$, obtained after the IFFT and P/S conversion in the OFDM modulator (figure 3.1), can be considered Rayleigh distributed. Additionally, the phase information $\text{Arg}\{b_x(t)\} = \alpha_x(t)$ can be considered as uniformly distributed in the interval $[-\pi, \pi]$. Statistical characterization of the non-linear distortion of an OFDM signal will be addressed more in detail in a later chapter to develop a special pre-distortion scheme.

Up to this point we have considered that no aliasing is introduced along the transmission stages. However, in real systems, operating at critical sampling rate will produce intolerable aliasing levels, specially when samples pass through the digital-analog converters. Moreover, spectral spreading of the base-band signal is expected due to the nonlinear nature of the HPA. Therefore, oversampling and filtering procedures must be suitably defined. We shall include some details regarding this after reviewing another important parameter that must be taken under consideration: the cyclic extension.

3.1.2 Guard Time and Cyclic Extension

One of the main properties that make OFDM appealing is its efficiency in counteracting multipath delay spread. In most OFDM applications a guard interval is inserted between OFDM base-band signal blocks to prevent intersymbol interference (ISI). This guard time is normally chosen larger than the expected delay spread so that multipath components from one symbol do not interfere with the next one. The guard itself will usually consist of a sub-set of null or zero-valued signals. However, in such cases, although ISI is already prevented by the inter-symbol distance, inter-carrier interference (ICI) may arise causing the subcarriers to lose orthogonality. Thence, to overcome the ICI problem, normally the OFDM symbol is cyclically extended along the guard time, so that any subcarrier coming from direct or delayed replicas of the signal will continue to have an integer number of cycles within an FFT interval of duration T. This ensures the orthogonality among the different subchannels as long as the delay remains smaller than the selected guard time. Normally, this cyclic extension (CE) is implemented in the form of a cyclic prefix (CP) as shown in figure 3.2, where the extended OFDM symbol interval $T_1 = T + T_{CE}$ is represented for only three separate subcarriers.

In figure 3.3 an example with three OFDM subcarriers is shown in order to illustrate how a suitable cyclic extension can help preserve orthogonality in the presence of multipath. In this particular example, the guard time is larger than the multipath delay

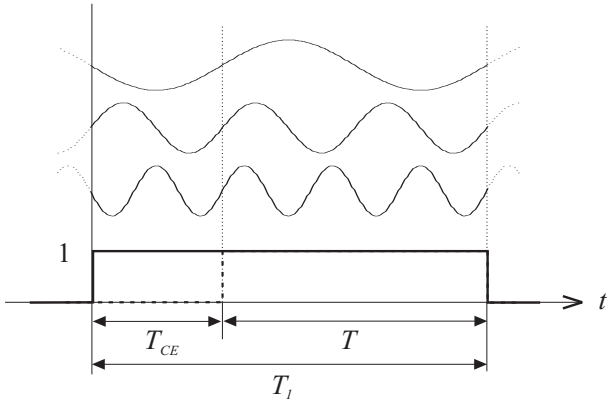

Figure 3.2: Cyclic extension and windowing for three OFDM subcarriers.

undergone by the OFDM signal. Thence, the OFDM receiver demodulates a sum of pure tone sine waves with uniform phase offsets, according to the transmitted symbol and the sum of their delayed replicas. Thus, during each FFT interval of duration T, the orthogonality between subcarriers is maintained, since no discontinuous phase transitions from the delayed path fall within any FFT integration interval.

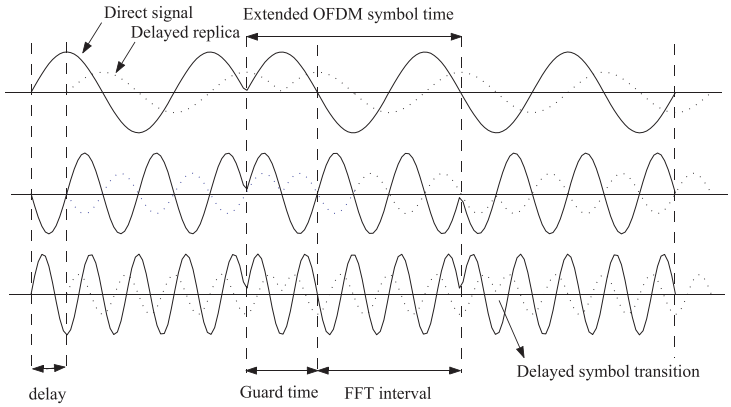

Figure 3.3: Three consecutive OFDM subcarriers modulated with BPSK during three symbol intervals. The cyclic extension of $T/2$ prevents the effect of the two-ray multipath at the receiver.

Along with the considerations regarding the multipath delay, we must note that the IFFT/FFT, evaluated for one OFDM symbol, will only preserve the desired orthogonality if the convolution in time between each separated subcarrier and the impulse response of its corresponding subchannel is cyclic rather than linear. In other words, as well as considering multipath delay, the guard time must be chosen larger than the maximum duration of impulse response among the N subchannels. In terms of frequency spectrum, this means that in OFDM the ICI is avoided since the maximum of any single subcarrier should correspond to the zero crossings of all the other carriers as shown in the example of figure 3.4, where the central spectrum has been highlighted to emphasize the orthogonality with respect to the other subcarriers.

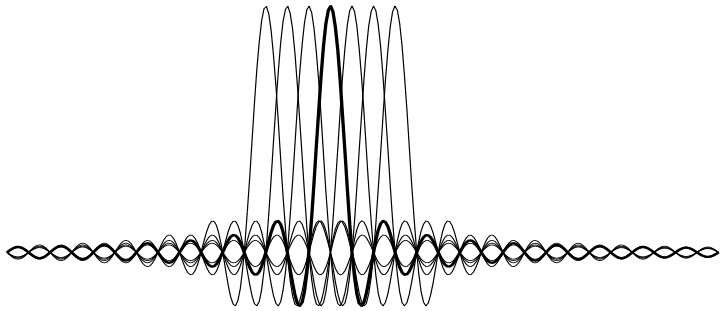

Figure 3.4: Orthogonal subcarriers spectrum.

In many OFDM designs, a guard interval approximately between 10% to 25% of the original symbol duration is employed [52]. In a HIPERLAN standard [4], for example, a cyclic prefix of duration $0.8\mu S$ (or optionally $0.4\mu S$) is copied from a $3.2\mu S$ useful symbol part to obtain a $4.0\mu S$ total symbol interval . Thus, the cyclic extension must not be understood as an exact periodic extension (PE). However, after removing the cyclic prefix from the received OFDM block, the N samples of the original symbol can be considered a basic periodic block, extracted from a virtual sequence of samples $\widetilde{b}_x[n]$ which is *infinite* and *periodic*. Thence, hereafter to refer to the cyclically extended version of any signal vector $\mathbf{x}$, we will use the notation $\overline{\mathbf{x}}$. We define the length of the discrete CE (in number of samples) as the integer N_{CE}. Thus, at critical sampling rate we have that $T_1 = T\frac{N_{CE}}{N}$.

The samples of the cyclically extended OFDM symbol in discrete-time are described from (3.3) by including a simple extension of the discrete window $w\,[\cdot]$,

$$\overline{b}_x[n] = \frac{1}{\sqrt{N}} \sum_{k=0}^{N-1} d_x[k] e^{j\frac{2\pi}{N}nk} w\,[n/(N + N_{CE} - 1)]\,. \tag{3.12}$$

Alternatively, we define the CE operation over the input vector $\mathbf{b}_x$ as

$$\overline{\mathbf{b}}_x = \mathbf{P}_\eta \mathbf{b}_x \tag{3.13}$$

where the CE operator $\mathbf{P}_\eta$ depends on the relation $\eta = \frac{N_{CE}}{N}$ which defines the following partitioned matrix:

$$\mathbf{P}_\eta = \begin{bmatrix} \mathbf{0}_{(N_{CE}\times N_\Delta)} & \mathbf{I}_{(N_{CE})} \\ \mathbf{I}_{(N)} & \end{bmatrix} \tag{3.14}$$

where $N > N_{CE}$ and $N_\Delta = N - N_{CE}$. Hence, in (3.13) this matrix adds the last N_{CE} samples of the original signal vector of length N to the front of the extended symbol, thus forming the cyclic prefix. Note that, in general, the dimensions of $\mathbf{P}_\eta$ will depend on the length of the vector to be extended. As we show in the next section, this will depend on whether the CE process takes place before (as in figure 3.1) or after signal oversampling.

3.1.3 Oversampling

In the previous expressions, the indexing of the elements from time-dependent vectors (for instance, n in $b_x[n]$) and the discrete-time evaluation using $(nT_s) = [n]$ coincide in denoting critical sampling at Nyquist rate. However, since oversampling should take place according to transmission hardware requirements, we must introduce the notation $x[n/L]$ to refer in general to the oversampling of the signal $x[n]$ by a factor L. Similarly, for the oversampled version of any vector $\mathbf{x}$ we will use the notation $\mathbf{x}_L$.

In the system shown previously in figure 3.1, the modulation stages operate at the critical sampling rate $f_s = N/T$. The corresponding transmission chain, including post-extension oversampling, is shown in figure 3.5 where an L-rate interpolator block is included to produce the cyclically extended and oversampled signal $\overline{\mathbf{b}}_{xL}$ which is then D/A converted, filtered and transmitted in RF. At this point we must recall that the effect of these transmission blocks (filters and D/A converters) will be discussed later, so that they are still assumed to perform ideally.

The time-domain interpolation shown in figure 3.5 normally consists on two steps: the insertion of $(L-1)$ zeros after each sample in the original sequence, and then a lowpass filtering of the resulting extended sequence. Thus, the vector at the output of the interpolator filter contains the unmodified original samples with $(L-1)$ interpolated values in between. Regardless of the cyclical extension, it is assumed that the spectrum

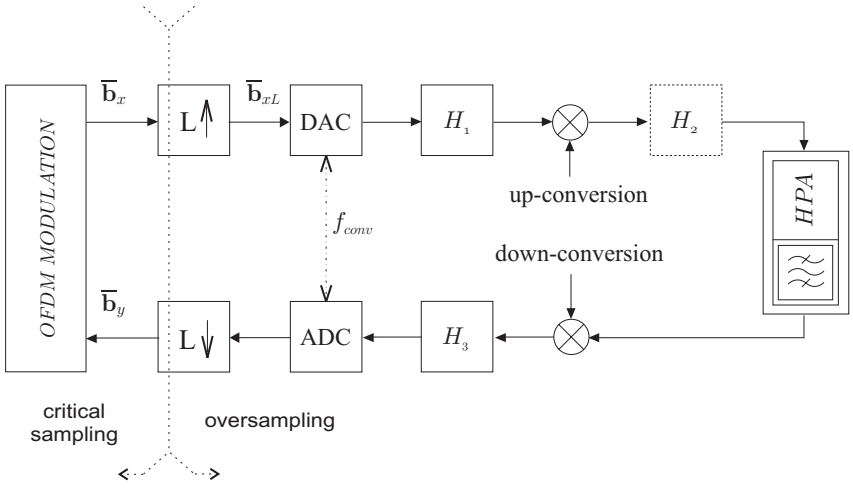

Figure 3.5: Transmission stages for figure 3.1, including oversampling by L.

of a well interpolated sequence $\mathbf{b}_{xL}$ is almost identical to the spectrum that would result from sampling the original signal $\mathbf{b}_x$ at an L-times higher sampling rate. In practice, an oversampled version of (3.3) can be obtained more efficiently through a frequency-domain interpolation, which can be implemented by zero padding the IFFT as shown in figure 3.6. This operation is expressed as follows:

$$b_{x[\frac{n}{L}]} = \frac{1}{\sqrt{N}} \sum_{k=0}^{N-1} d_x[k] e^{j\frac{2\pi}{NL}nk} w[n/(NL-1)] \tag{3.15}$$

$$= \frac{1}{\sqrt{N}} \left(\sum_{k=0}^{\frac{N}{2}-1} d_x[k] e^{j\frac{2\pi}{NL}nk} + \sum_{k=NL-\frac{N}{2}}^{NL-1} d_x[k-N(L-1)] e^{j\frac{2\pi}{NL}nk} \right) w[\frac{n}{(NL-1)}] \tag{3.16}$$

$$= \text{IDFT}\Big[\, d_x[0] \dots d_x[N/2-1] \underbrace{0 \dots 0}_{N(L-1)} d_x[N/2] \dots d_x[N-1] \,\Big] = \text{IDFT}\left(\mathbf{d}_{x_{zp}}\right) \tag{3.17}$$

thus, the oversampled OFDM symbol vector $\mathbf{b}_{xL} = \left[b_x[\frac{0}{L}] \cdots b_x[\frac{NL-1}{L}]\right]^T$ is given by

$$\mathbf{b}_{xL} = \mathbf{F}^{\text{H}} \mathbf{d}_{x_{zp}}. \tag{3.18}$$

Note that the size of the FFT matrix, defined in (3.6), must depend on the length of the vectors involved in each transformation. According to this, in (3.18) the matrix dimensions correspond to $(NL \times NL)$. At the increased sampling rate $f_{os} = Lf_s$, the length of the discrete CE is now $N_{Lce} = N_{CE}L$ samples, while its equivalent time-domain span is still $T_{CE} = N_{CE}\frac{T}{N}$. Then, the oversampled version of the cyclically extended symbol in (3.12) is obtained with

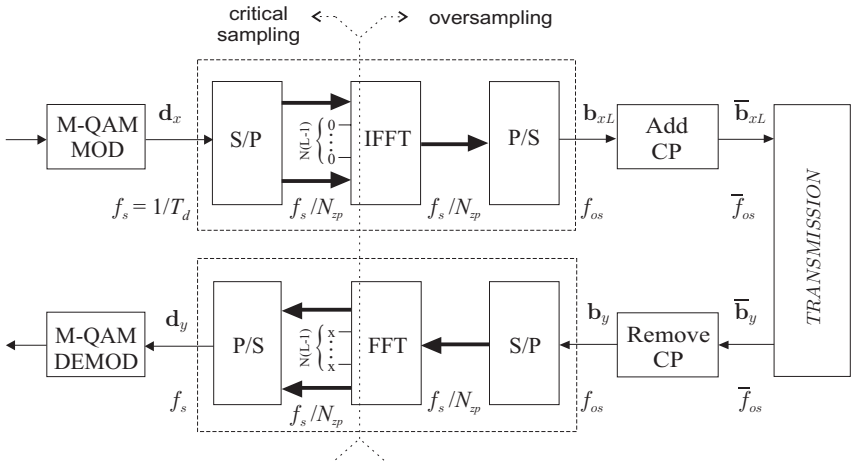

Figure 3.6: Block diagram of the OFDM modulation stages including $N(L-1)$ zero padding at IFFT.

$$\overline{b}_x[n/L] = \frac{1}{\sqrt{N}} \sum_{k=0}^{N-1} d_x[k] e^{j\frac{2\pi}{NL}nk} w[n/\left(L(N+N_{CE})-1\right)]. \tag{3.19}$$

Equivalently, using the CE operator defined in (3.14), the corresponding output vector for transmission can be expressed as

$$\overline{\mathbf{b}}_{xL} = \mathbf{P}_\eta \mathbf{F}^{\mathrm{H}} \mathbf{d}_{x_{zp}} \tag{3.20}$$

where the extention ratio is specifically $\eta = \frac{N_{Lce}}{NL}$. This leads to larger CE matrix dimensions but maintains the relative value of the CE over the oversampled signal vector length.

Once these basic topics concerning the signal generation have been described, we will focus our attention on reviewing some important aspects on the frequency-domain representation of the signal and the nonlinear distortion phenomenon. According to classical modeling rules, the superposition principle does not hold for nonlinear systems and therefore the nonlinear part of such systems is expected to be simulated only in time domain. However, the particular OFDM signal structure strongly suggests that the analysis of frequency domain approaches is necessary to deduce and support system modeling criteria and to expand our viewpoints in the search for new digital processing solutions.

3.2 Analysis of the Frequency Domain Representation of the Signal

In this section we analyze some details on the frequency-domain representation of the signal model previously presented. The aim is to take advantage of the particular OFDM signal structure, to analytically describe the effect of nonlinear distortion and to find suitable conditions for its compensation. Since digital pre-distortion is expected to perform in discrete time-frequency domain, aspects like invertibility conditions and discrete representation of analog stages should be also discussed in this first approach. Complementary with the general Volterra Series Model (time domain), which is presented in section 2.1, here we also derive the formulation of an analytical model for the characterization of nonlinear distortion using a multidimensional frequency-convolution based expansion.

3.2.1 Analog Spectral Representation

According to the general definitions given in section 3.1.1, each independent OFDM symbol must contain a combination of pure-tone complex subcarriers located at $f_k = \{0, \frac{1}{T}, \frac{2}{T}, \ldots, \frac{(N-1)}{T}\}$. Letting the symbol $\mathbf{b}_x$ extend far beyond the period T, so as to produce a *periodic signal*, provides an ideal analog generation of a permanent OFDM symbol. Such periodic extention of the signal will be denoted as $\widetilde{b}_x(t)$. In frequency domain this simplified model can be expressed in the form

$$\widetilde{X}(f) = \sum_{k=0}^{N-1} d_k \, \delta\left(f - \frac{k}{T}\right) \quad ; \quad 0 \leq k \leq N-1 \tag{3.21}$$

where d_k are the complex coefficients M-QAM (included as $d_x[k]$ in eq.(3.3)) that convey the amplitude and phase information that modulates each subcarrier within one OFDM symbol. In general, we will consider that in one extended OFDM symbol, the subcarriers are windowed (multiplied) in continuous time with a unitary amplitude rectangular pulse $w(t/T_p)$ of duration T_p which is defined by

$$w(t/T_p) = \begin{cases} 1 & ; \quad 0 \leq t \leq T_p \\ 0 & ; \quad \text{otherwise} \end{cases} \tag{3.22}$$

as we similarly defined for discrete time in equation (3.4). The frequency spectrum for this continuous time unitary rectangular pulse is given by its Fourier Transform

$$W(f) = T_p \, \frac{\sin(\pi T_p f)}{\pi T_p f} e^{-jT_p \pi f} = T_p \, \mathrm{sinc}(T_p f) e^{-jT_p \pi f} \tag{3.23}$$

where the phase term $e^{-jT_p\pi f}$ becomes null if the pulse is centered at the interval $t = \pm T_p/2$. Using (3.23), the spectrum $X(f)$ of a single OFDM symbol for a given interval $\mathcal{I}_i = [iT_p, iT_p + T_p]$, can be expressed in a simplified way as the frequency-domain convolution between the window $W(f)$ and the group of N Dirac pulses (OFDM subcarriers),

$$\begin{aligned} X(f) &= W(f) * \sum_{k=0}^{N-1} d_k\, \delta\left(f - \frac{k}{T}\right) = \sum_{k=0}^{N-1} d_k\, W\left(f - \frac{k}{T}\right) \\ &= T_p \sum_{k=0}^{N-1} d_k\, \mathrm{sinc}\left(T_p\left(f - \frac{k}{T}\right)\right) e^{-jT_p\pi\left(f-\frac{k}{T}\right)}. \end{aligned} \tag{3.24}$$

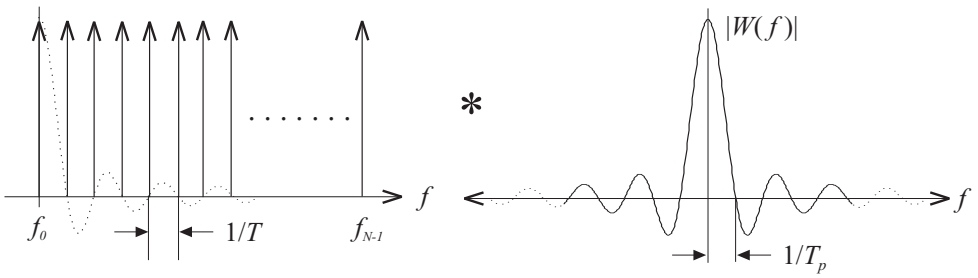

Figure 3.7: Frequency domain equivalent for the time windowing of OFDM subcarriers given by the convolution of deltas located at f_k and the FT of a square window of duration T_p. The dotted plot on the left shows the adequate frequency spacing relation ($T = T_p$) to obtain orthogonality

This operation is represented in figure 3.7 only in terms of amplitude spectrum and considering d_k as constant amplitude modulation data (QAM). From this figure, we can easily observe that only for windows of duration $T_p = \{T, 2T, 3T, \ldots\}$, –which is called a "periodic extension" (PE) of the symbol–, the evaluation of (3.24) will result in a well distributed pattern of *orthogonal* subcarriers. This dependence of the orthogonality between spectra from the FFT window length is shown in figure 3.8 for two different values of T_p (see also figure 3.2 where the case $T_p = T$ appears as a dotted line). Note that in figures 3.7 and 3.8 the phase shifting term $e^{-jT_p\pi f}$ associated to each 'sinc' spectrum is not beign considered, so that only amplitude spectrums are represented.

The definition of one independent OFDM symbol implies that the subcarriers should be declared null when out of the corresponding interval of duration T. Nevertheless, in practice the system will transmit the cyclically extended symbol $\overline{\mathbf{b}}_x$ where these N components are no longer orthogonal, although they remain centered at the same frequencies f_k as shown in figure 3.8b. Therefore, in the reception branch, the samples of the cyclic extension (CE) must be discarded to re-create the original OFDM symbol, thus obtaining a periodic-like signal block (integer number of cycles for each subcarrier) for the FFT to process. Furthermore, windowing the received frame by T is required to restore the orthogonality between subcarriers before demodulation. Nevertheless, removing the CE (along with the use of a guard time which is discussed later) implies a

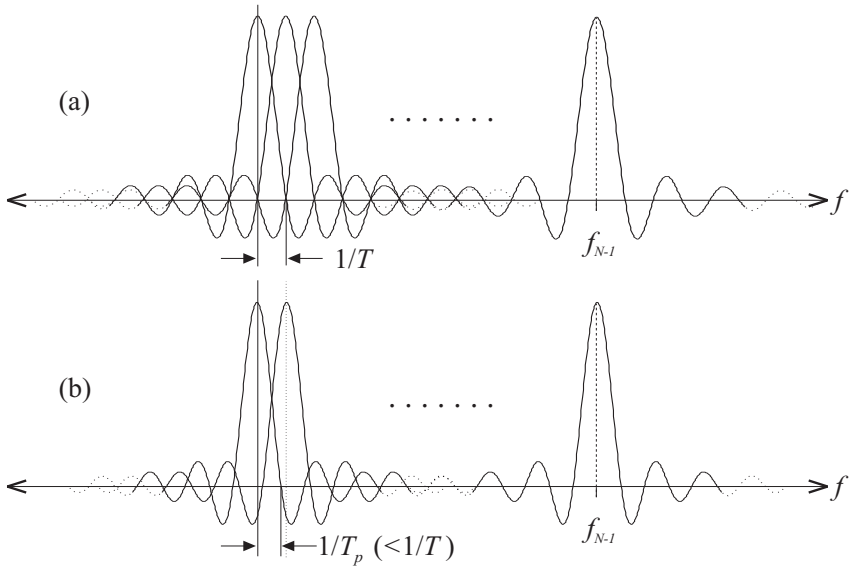

Figure 3.8: Comparison between OFDM spectra using two different values for the window that define the FFT interval. (a)using $T_p = T$ results in orthogonality (b)using $T_p > T$ the subcarriers are no longer orthogonal.

certain cost in terms of SNR. Thus, processing the CE leads to a better spectral efficiency but at the cost of an increased processing complexity.

Up to this point, we have characterized the undistorted input to the HPA. The next important step is to describe the changes undergone by the signal spectrum when it is distorted with a nonlinear device. Therefore, in the next subsection, the input-output relationship of a simple memoryless non-linear HPA is analyzed through an analog frequency domain approach based on an analytical spectral representation of the nonlinear distortion effects.

3.2.2 Spectral Modeling of the Non-Linear Transference

We are now concerned with the frequency domain representation of the nonlinear distortion. This first analog scheme aims to characterize the effect of the HPA over the OFDM signal spectrum, which is intended to help develop an equivalent discrete representation in later sections.

The basic representations of the OFDM signal given by (3.21) and (3.24) are well suited analog expressions for our analytical modeling purposes. Nevertheless, we shall start with a more general expression for the same input base-band signal and its corresponding

spectrum,

$$b_x(t) \overset{FT}{\longleftrightarrow} X(f) = \int_{-\infty}^{\infty} b_x(t) e^{-j2\pi ft} dt.$$

Along with this, the inverse FTs of $b_x(t)$ and its complex conjugated are respectively

$$b_x(t) = \int_{-\infty}^{\infty} X(f) e^{j2\pi ft} df$$

$$b_x^*(t) = \int_{-\infty}^{\infty} X^*(-f) e^{j2\pi ft} df$$

while the squared modulus of the signal has the following correspondence:

$$u_x^2(t) = b_x(t)\ b_x^*(t) = |b_x(t)|^2 \overset{FT}{\longleftrightarrow} X(f) * X^*(-f) = r_{xx}(f)$$

where $r_{xx}(f)$ corresponds to the autocorrelation of the signal spectrum $X(f)$.

In accordance with these definitions, a reasonable choice is to consider that the HPA's base-band nonlinearity can be modeled as an amplitude-dependent multiplicative gain according to

$$G(u_x^2(t)) = \sum_{q=0}^{\infty} g_q u_x^{2q}(t) \tag{3.25}$$

where the functional dependence of the gain model is restricted to even powers of $u_x(t)$. This is rather logical since we normally intend to provide an input-output model for the first zone output of the HPA [1]. This means that only odd power nonlinear terms should be contained in the series model of the nonlinear HPA output which is given by,

$$b_y(t) = b_x(t) \sum_{q=0}^{\infty} g_q u_x^{2q}(t) \tag{3.26}$$

where, recalling that $b_y(t) = u_x(t) e^{j\alpha_x(t)}$, it becomes clear that (3.26) contains only odd-power components.

The evaluation of the time-frequency correspondence for a given set of even powers of the base-band envelope $u_x^{2q}(t)$ for $q = \{1, 2, 3, \ldots\}$, leads us to the following recursive definition:

[1] Components of the normalized output spectrum for the interval $\omega = [0, 2\pi]$.

$$\begin{array}{ccc} u_x^2(t) & \overset{FT}{\longleftrightarrow} & X(f) * X^*(-f) = r_{xx}^{(1)}(f) \\ u_x^4(t) & \overset{FT}{\longleftrightarrow} & r_{xx}^{(1)}(f) * r_{xx}^{(1)}(f) \equiv r_{xx}^{(2)}(f) \\ u_x^6(t) & \overset{FT}{\longleftrightarrow} & r_{xx}^{(2)}(f) * r_{xx}^{(1)}(f) \equiv r_{xx}^{(3)}(f) \\ \vdots & \vdots & \vdots \\ u_x^{2q}(t) & \overset{FT}{\longleftrightarrow} & r_{xx}^{(q-1)}(f) * r_{xx}^{(1)}(f) \equiv r_{xx}^{(q)}(f) \end{array} \tag{3.27}$$

which is completed by defining $r_{xx}^{(0)}(f) = 1$. Then, from (3.26) we can express the PSD for the base-band output of the HPA as,

$$Y(f) = X(f) * \sum_{q=0}^{\infty} g_q r_{xx}^{(q)}(f). \tag{3.28}$$

Here, the nonlinear distortion is expressed in frequency domain as the convolution of the input signal spectrum $X(f)$ with the infinite summation of q-order spectral autocorrelations, each one associated with a complex coefficient g_q that act like weights for intermodulation products. To express the first-order spectral autocorrelation, we use (3.24) obtaining

$$r_{xx}^{(1)}(f) = X(f) * X^*(-f) = \sum_{k=0}^{N-1} d_k W\left(f - \frac{k}{T}\right) * \sum_{k'=0}^{N-1} d_{k'} W^*\left(-f + \frac{k'}{T}\right). \tag{3.29}$$

Now, since from (3.23) we can observe that the window spectrum exhibits hermitian symmetry

$$W^*(-f) = T_p \,\mathrm{sinc}(-T_p f) e^{jT_p\pi(-f)} = T_p \,\mathrm{sinc}(T_p f) e^{-jT_p\pi f} = W(f), \tag{3.30}$$

equation (3.29) becomes

$$r_{xx}^{(1)}(f) = \underbrace{\sum_{k,k'}}_{N^2\text{elements}} d_k d_{k'}^* W\left(f - \frac{k}{T}\right) * W\left(f - \frac{k'}{T}\right). \tag{3.31}$$

For further simplification, note that the convolution of the frequency shifted windows spectra in (3.31), which will be denoted as $r_{ww}(f,k,k')$, can be reduced as follows:

$$\begin{aligned} r_{ww}(f,k,k') &= W\left(f - \frac{k}{T}\right) * W\left(f - \frac{k'}{T}\right) = W(f) * W\left(f - \frac{k+k'}{T}\right) \\ &= T_p^2 \int_{-\infty}^{\infty} \mathrm{sinc}\Big(T_p\tau\Big) e^{-jT_p\pi\tau} \mathrm{sinc}\Big(T_p(f - \frac{k+k'}{T} - \tau)\Big) e^{-jT_p\pi(f - \frac{k+k'}{T} - \tau)} d\tau \\ &= T_p^2 e^{-jT_p\pi(f - \frac{k+k'}{T})} \int_{-\infty}^{\infty} \mathrm{sinc}\Big(T_p\tau\Big) \mathrm{sinc}\Big(T_p(f - \frac{k+k'}{T} - \tau)\Big) d\tau \end{aligned} \tag{3.32}$$

and introducing the change of variable $\psi = T_p\tau$,we have

$$\begin{aligned} r_{ww}(f,k,k') &= T_p\, e^{-jT_p\pi(f-\frac{k+k'}{T})} \int_{-\infty}^{\infty} \mathrm{sinc}\Big(\psi\Big)\mathrm{sinc}\Big(T_p(f-\frac{k+k'}{T})-\psi\Big)d\psi \\ &= T_p\, e^{-jT_p\pi(f-\frac{k+k'}{T})}\, \mathrm{sinc}\Big(T_p(f-\frac{k+k'}{T})\Big) \\ &= W\left(f-\frac{k+k'}{T}\right). \end{aligned} \tag{3.33}$$

Thence, using (3.33) in (3.31) yields

$$r_{xx}^{(1)}(f) = \sum_{k,k'} d_k d_{k'}^* W\left(f-\frac{k+k'}{T}\right). \tag{3.34}$$

By introducing a new variable $\delta = k + k'$ in this last expression, we can rewrite it as

$$r_{xx}^{(1)}(f) = \sum_{\delta=0}^{2N-2}\left[\sum_{k+k'=\delta} d_k d_{k'}^*\right] W\left(f-\frac{\delta}{T}\right) \tag{3.35}$$

where the summation term in square brackets corresponds to a discrete convolution of the subcarriers information (M-QAM), i.e., the sum of possible intermodulation products associated to the same phase shift δ/T. This term can be suitably redefined as

$$D_\delta = \sum_{k+k'=\delta} d_k d_{k'}^* \text{ ; for } \delta = \{0,1,2,3,\ldots,2N-3,2N-2\}. \tag{3.36}$$

Extending the evaluation of (3.36) for all the different values of δ we have,

$$\left.\begin{array}{lcl} D_0 & = & d_0 d_0^* \\ D_1 & = & d_0 d_1^* + d_1 d_0^* \\ D_2 & = & d_0 d_2^* + d_1 d_1^* + d_2 d_0^* \\ D_3 & = & d_0 a_3^* + d_1 a_2^* + d_2 d_1^* + d_3 d_0^* \\ & \vdots & \\ D_{N-1} & = & d_0 d_{N-1}^* + d_1 d_{N-2}^* + d_2 d_{N-3}^* + \ \ldots\ + d_{N-2} d_1^* + d_{N-1} d_0^* \end{array}\right\} \tag{3.37}$$

$$\left.\begin{array}{lcl} D_N & = & d_1 d_{N-1}^* + d_2 d_{N-2}^* + d_3 d_{N-3}^* + \ldots + d_{N-2} d_2^* + d_{N-1} d_1^* \\ D_{N+1} & = & d_2 d_{N-1}^* + d_3 d_{N-2}^* + \ldots + d_{N-2} d_3^* + d_{N-1} d_2^* \\ & \vdots & \\ D_{2N-3} & = & d_{N-2} d_{N-1}^* + d_{N-1} d_{N-2}^* \\ D_{2N-2} & = & d_{N-1} d_{N-1}^*. \end{array}\right\} \tag{3.38}$$

From (3.37) and (3.38) we can extract two different recursion rules that define the computation of D_δ in (3.36) as the following piece-wise equation:

$$D_\delta = \begin{cases} \sum_{\ell=0}^{\delta} d_\ell \, d^*_{\delta-\ell} & ; \quad \text{for } 0 \le \delta \le N-1 \\ \\ \sum_{\ell=\delta-(N-1)}^{N-1} d_\ell \, d^*_{\delta-\ell} & ; \quad \text{for } N \le \delta \le 2N-2. \end{cases} \tag{3.39}$$

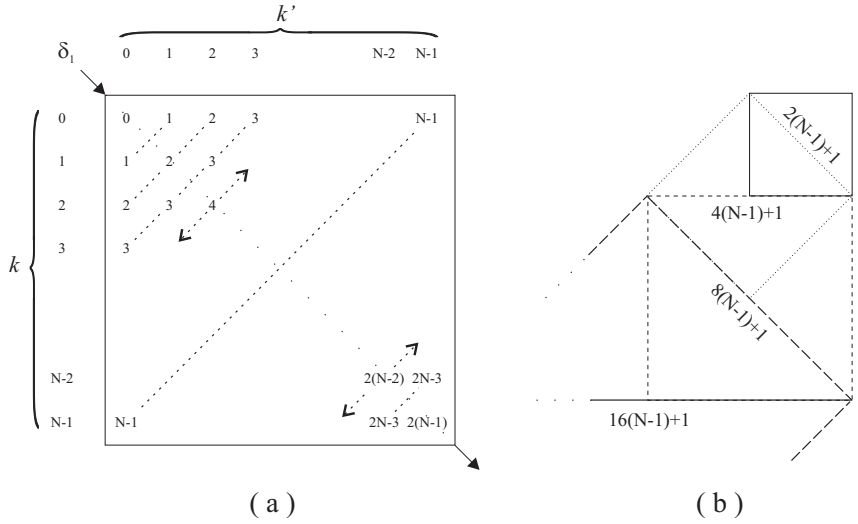

Figure 3.9: (a) Square array with all possible combinations for $k+k'$. The size $(N \times N)$ defines $2(N-1)+1$ equipotential lines across the main diagonal for q=1.(b) The recursion analysis defines $2q(N-1)+1$ equipotential lines (values for δ_q) when $q = \{1, 2, 4, 8, 16, \ldots, 2^n\}$.

This compact expression helps us evaluate the spectral autocorrelation included in (3.28) for different values of q so that we may search for a single expression for $r^{(q)}_{xx}(f)$. Thus, for $q = 1$ we have,

$$r^{(1)}_{xx}(f) = \sum_{\delta_1=0}^{2N-2} D^{(1)}_{\delta_1} W(f - \frac{\delta_1}{T}) \tag{3.40}$$

where $D^{(1)}_{\delta_1}$ is calculated using (3.39). The reason for the super index is to specify the order q, likewise we include the sub index in $\delta_1 = k + k'$. Additionally, since k and k' in (3.35) could take any values within the range $\{0, \ldots, N-1\}$, we show in figure (3.9) a graphical representation spanning all the combinatorial results for the sum $k + k'$ which could be helpful in establishing the recursive relationship we are looking for. Then, for

$q = 2$,

$$\begin{aligned} r_{xx}^{(2)}(f) &= r_{xx}^{(1)}(f) * r_{xx}^{(1)}(f) = \sum_{\delta_1=0}^{2N-2} D_{\delta_1}^{(1)} W(f - \frac{\delta_1}{T}) * \sum_{\delta_1'=0}^{2N-2} D_{\delta_1'}^{(1)} W(f - \frac{\delta_1'}{T}) \\ &= \sum_{\delta_2=0}^{2(2N-2)} \sum_{\delta_1+\delta_1'=\delta_2} [D_{\delta_1}^{(1)} D_{\delta_1'}^{(1)}]\, W(f - \frac{\delta_2}{T}) = \sum_{\delta_2=0}^{2(2N-2)} D_{\delta_2}^{(1)} W(f - \frac{\delta_2}{T}) \end{aligned} \quad (3.41)$$

and similarly,

$$\begin{aligned} r_{xx}^{(4)}(f) &= r_{xx}^{(2)}(f) * r_{xx}^{(2)}(f) = \sum_{\delta_2=0}^{2(2N-2)} D_{\delta_2}^{(2)} W(f - \frac{\delta_2}{T}) * \sum_{\delta_2'=0}^{2(2N-2)} D_{\delta_2'}^{(2)} W(f - \frac{\delta_2'}{T}) \\ &= \sum_{\delta_4=0}^{4(2N-2)} \sum_{\delta_2+\delta_2'=\delta_4} [D_{\delta_2}^{(2)} D_{\delta_2'}^{(2)}]\, W(f - \frac{\delta_4}{T}) = \sum_{\delta_4=0}^{4(2N-2)} D_{\delta_4}^{(4)} W(f - \frac{\delta_4}{T}). \end{aligned} \quad (3.42)$$

The recursion rule to obtain D_{δ_q}, when $q = \{1, 2, 4, 8, 16, \ldots, 2^n\}$, can be expressed in the following constrained form:

$$D_{\delta_q}^{(q)} = \begin{cases} \sum\limits_{\delta_{q'}=0}^{\delta_q} D_{\delta_{q'}}^{(q')}\, D_{\delta_q-\delta_{q'}}^{(q')} & ; \quad \text{for } 0 \le \delta_q \le q(N-1) \\ \sum\limits_{\delta_{q'}=\delta_q-q(N-1)}^{q(N-1)} D_{\delta_{q'}}^{(q')}\, D_{\delta_q-\delta_{q'}}^{(q')} & ; \quad \text{for } q(N-1)+1 \le \delta_q \le 2q(N-1) \end{cases} \quad (3.43)$$

where is important to note that $q' = q/2$. This expression is only suited for those q that are powers of two. Thus, using (3.43), the analytical expression of the spectral autocorrelation can be expressed as

$$r_{xx}^{(q)}(f) = r_{xx}^{(\frac{q}{2})}(f) * r_{xx}^{(\frac{q}{2})}(f) = \sum_{\delta_q=0}^{q(2N-2)} D_{\delta_q}^{(q)} W(f - \frac{\delta_q}{T}) \quad (3.44)$$

for any $q = 2^n$, with $n = \{1, 2, 3, 4, \ldots\}$. In order to make (3.44) extensive for any $q = \{1, 2, 3, 4, 5, 6, 7, 8, \ldots\}$, we resort to a decomposition of the q-order autocorrelation into a multi-convolution of 2^n-order autocorrelations through the identity

$$r_{xx}^{(q)} = r_{xx}^{(2^{PQ})} * \cdots * r_{xx}^{(2^{P3})} * r_{xx}^{(2^{P2})} * r_{xx}^{(2^{P1})} * r_{xx}^{(2^{P0})} \quad ; \sum_{p=(P0,\ldots,PQ)} 2^p = q \quad (3.45)$$

which simply corresponds to the binary decomposition of the exponent q.

The analog representation of the signal spectrum and the characteristics of its non-linear transference are just a theoretical basis for the following analysis since in practice any PD process will perform in discrete domain. Moreover, discrete representation parameters shall be determined so as to ensure reliability and accuracy in the discrete equivalent representation of analog stages within the transmission chain.

3.3 Schemes for Discrete Domain Representation

In this section a number of aspects concerning the discrete representation of the system and the signal model are reviewed. As previously seen, the OFDM system is characterized by an hybrid time-frequency structure where the HPA's nonlinear distortion and its linearization stages are expected to perform in discrete domain. Therefore, the following analysis will be particularly focused on the discrete representation of the analog stages involved in the signal transmission process. For this purpose, we develop here a purely deterministic treatment, where the analysis is limited to the transmission of a single OFDM symbol and/or its various extensions. We aim to characterize the signal evolution through the processing chain and provide a suitable description of how the M-QAM symbols are transmitted on the multi-carrier pattern support.

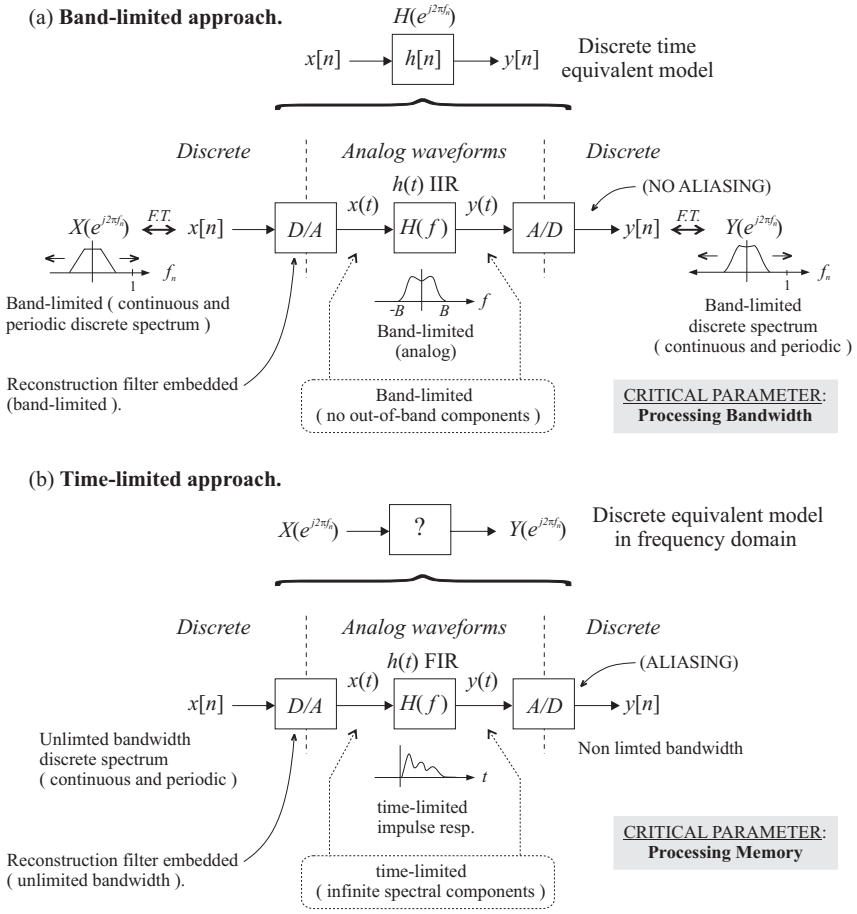

Figure 3.10: Contrasted approaches to obtain a discrete equivalent model.

3.3.1 Preliminary discussion

In figure 3.10 we represent two different approaches that can be considered as counterparts for a preliminary discussion on how to define our discrete modeling scenario. The objective here can be stated in general as the development of an equivalent discrete model to faithfully represent the analog transference of a discrete input $x[n]$ through an analog channel $H(f)$ and finally obtain the discrete output $y[n]$. The function $H(f)$ can be defined so as to represent the combined frequency response of several stages in the chain (such as filters and channel selectivity) in a single linear time-invariant (LTI) analog subsystem. Under these conditions, however, a modeling problem will arise with the eventual inclusion of nonlinear blocks in the chain. One of these nonlinearities is the HPA itself, which is placed among analog stages although it is ultimately modeled in discrete domain, and another such nonlinearity is the PD processor, which will be included before the D/A conversion at the transmitter.

For LTI systems the common approach for the discrete representation of the transmission process, involving the signal model and equivalent system representation, is to consider a band-limited process (figure 3.10(a)) where the FT of the continuous signal is strictly conditioned to be $X(f) = 0$ for $|f| > B$ at every point within the chain. Along with this, assuming that each analog subsystem is also band-limited and with the sampling rate f_s fulfiling the sampling theorem requirements (i.e. Nyquist sampling at $f_s \geq 2B$), signal reconstruction can be performed without any aliasing. The D/A conversion is thus based on ideal interpolation of the samples using 'sinc' functions, which is equivalent to restoring the continuous signal through ideal low-pass filtering. Note that such filter should have an infinite impulse response such as $h(t) = (\sin(2\pi Bt))/(2\pi Bt)$. Thence, two critical limiting factors for the applicability of this band-limited assumptions can be pointed out:

- The band-limited frecuency response of analog stages is associated with an impulse response of infinite duration. Then, to convert the analog transference $y(t) = h(t) * x(t) = \int_{-\infty}^{\infty} h(\tau)x(t-\tau)d\tau$ to its eventual discrete equivalent model, a discrete convolution $y[n] = h[n] * x[n] = \sum_{m=-\infty}^{+\infty} h[m]x[n-m]$ must be performed with an infinite duration $h[n]$. Then, the infinite summation can be circumvented by using circular convolution if the input $x[n]$ is periodic.
- A band-limited model is inadequate to include nonlinearities. Any subsystem including nonlinearities introduces an important spectral regrowth (SR) and its output will theoretically have an infinite bandwidth. Thence, discarding the out-of-band information would critically affect signal reconstruction and the linearization process since the pre-distorted signal spectrum conveys useful information in components that are far beyond the bandwidth of the original signal.

This latter drawback may be sufficient for us to consider the time-limited approach of figure 3.10(b) more adequate than the former band-limited assumptions. Nevertheless, it

is also worthy to consider that a normal practice in simulating communication systems is the use of a single sampling frequency for the whole chain. In such conditions the sampling rate should be determined with regard to the subsystem having the largest bandwidth. Thus, any subsystem including nonlinearities will be highly related to the determination of this equivalent maximum bandwidth and thence to the sampling rate associated to the system. Then, we can note that processing of strictly band-limited signals will require careful attention with the "processing bandwidth" as the critical parameter for modeling. Higher sampling frequencies are normally a stringent factor regarding real systems limitations. In contrast, when no bandwidth constraint is defined for the signal model and system design, the "processing memory" becomes the new critical parameter. Thus, a reliable discrete representation can be achieved with lower sampling frequency values with respect to the main band of the signal whenever the processing memory is larger than the limited time-span assumed for the system. Hence, since the processing memory is a less limited resource than the operating frequency for real implementations, the time-limited approach seems to be the reasonable choice for modeling the transference of a signal with well-defined time characteristics and including nonlinear effects. Some crucial comments regarding figure 3.10(b), where the time-limited approach is represented, are the following:

- Using this approach, the time-limited impulse response $h(t)$ associated with an infinite bandwidth for $H(f)$, could be represented through a discrete equivalent model where the interpolation of sequences can now be performed in frequency domain using 'sinc' functions.

- According to the time-limited assumption, the input and output signals at $H(f)$ are theoretically of infinite frequency span. This unlimited bandwidth, considered at the input of the A/D block, implies that the discrete output sequence $y[n]$ will incorporate aliasing components that shall be identified in the model.

- Additionally, any nonlinear block added to the linear chain will introduce an infinite number of spectral components. In particular, if the input signal $x[n]$ is a pre-distorted signal, it will present a widely spread frequency distribution with infinite spectral components. Then, the reconstruction filter embedded in the D/A converter must also be considered non-bandlimited.

Thus, using this second approach a theoretical equivalent discrete model can be found, which is in fact the aim of this section. However, it is evident that none of these two approaches could be efficiently implemented for modeling real systems, unless some restrictions are applied. The duality of the modeling criterion shall be solved through a trade off between time (processing memory) and bandwidth restrictions (processing bandwidth) in order to reduce simulation complexity at the lowest cost in parameter accuracy.

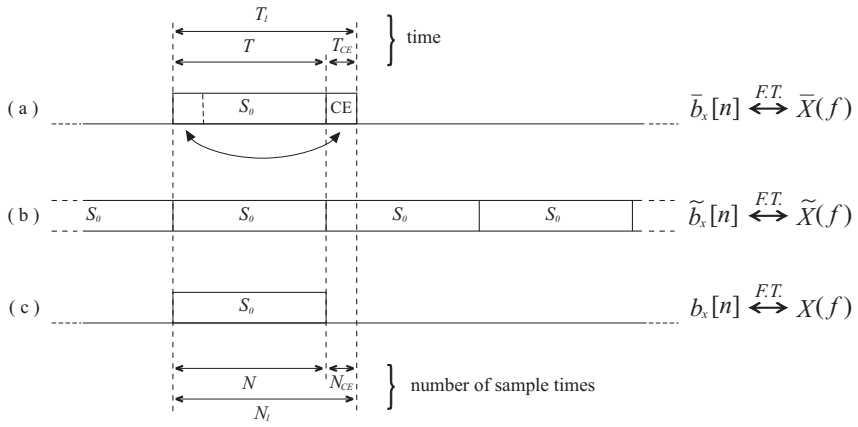

Figure 3.11: (a) Samples of the OFDM symbol with cyclic extension (b) periodically extended discrete signal (c) original OFDM symbol with the N M-QAM data samples.

3.3.2 Time–Frequency definitions and discrete signal structure.

From the deterministic structure of the analog input spectrum to the HPA, previously given in (3.24), the information that completely defines the base-band input signal and its spectrum is contained in the set of M-QAM data $\mathbf{d}_x$. This suggests the formulation of a suitable equivalent discrete model that encompasses all the stages in the transmission chain up to the demodulation of the base band information at the receiving end. The general scheme for discrete time-frequency representation will first be discussed and then an exact equivalent discrete model for signal transmission will be presented.

To start, it is convenient to recall the different versions of the signal that we have defined and mentioned up to this point (see figure 3.11):

$\mathbf{b}_x$ the available originally sampled symbol with length N,
$\overline{\mathbf{b}}_x$ the cyclically extended symbol with length $N + N_{CE}$, and
$\widetilde{b}_x(t)$ the periodic extension of the OFDM symbol also denoted $\widetilde{b}_x[n]$.

A scheme of these related signal definitions is shown in figure 3.11. A more complete scheme appears in a later discussion, including a new auxiliar signal frame and windowing definitions. The goal will be to find a suitable discrete spectral representation of $\overline{\mathbf{b}}_x$ taking into account a minimum sampling criterion (sampling theorem) so that the D/A reconstruction and filtering processes are not affected by the discrete windowing of the signal.

Let us consider first the FT for the original OFDM symbol $\mathbf{b}_x = \Big[b_x[0] \cdots b_x[N-1]\Big]^T$,

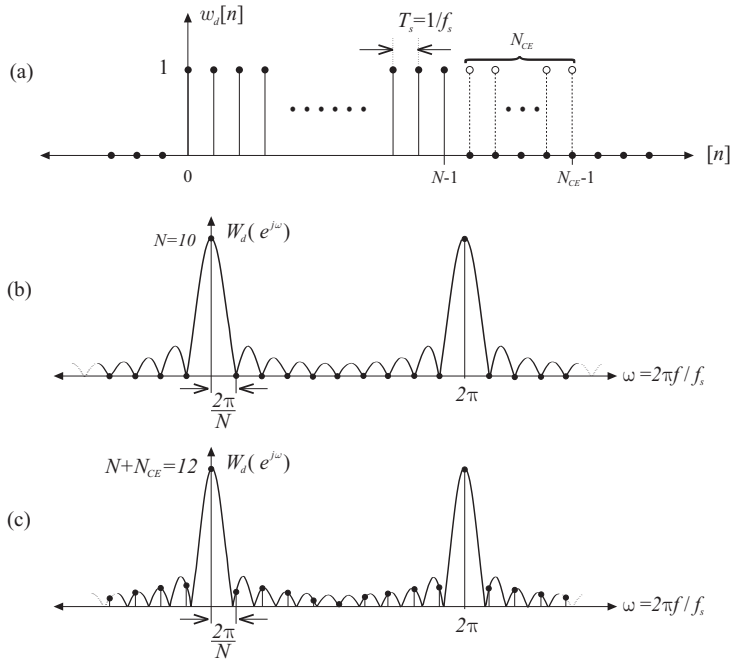

Figure 3.12: (a) Sample set in discrete time and (b) amplitude spectrum for the sampled rectangular window of height 1 with $N = 10$ and (c)with $N + N_{CE} = 12$. The dots show the discretized spectra whose samples are in both cases separated by $\Delta\omega = \frac{2\pi}{N}$. Note that, unlike the spectrum in (b), for the extended window with length $N + N_{CE} = 12$, the sampling points at $\omega = k\frac{2\pi}{N} \neq 2\pi m$ do not coincide with the nulls in (c).

whose elements were defined in (3.3). By definition of the FT of a discrete sequence, we have

$$X(e^{j\omega}) = \mathcal{F}(\mathbf{b}_x) = \sum_{n=-\infty}^{\infty} b_x[n]e^{-jn\omega} = \sum_{n=0}^{N-1} b_x[n]e^{-jn\omega} \tag{3.46}$$

where the parameter

$$\omega = 2\pi\frac{f}{f_s} = 2\pi f_n \tag{3.47}$$

is the normalized angular frequency with respect to the sampling rate $f_s = 1/T_s$. This frequency normalization will apply henceforth to refer to the dependence of the FT of discrete signals on the complex variable $e^{j\omega}$. Unless otherwise stated, it will be assumed that the signal samples of the base-band signal are acquired at $f_d = 1/T_d$, i.e., the same generation rate of the M-QAM data at the modulator (no oversampling).

The sampled version of a single OFDM symbol $\mathbf{b}_x$ can be obtained from the periodic signal $\widetilde{b}_x(t)$ whose spectrum, as seen previously in (3.21), consists of N pure tone

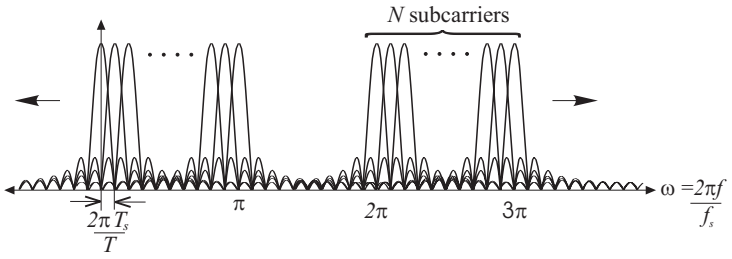

Figure 3.13: OFDM spectrum for a discrete window of length $2N$ and using twice the critical sampling rate.

subcarriers (analog deltas). Hence, we consider the windowing transform pair

$$\mathbf{b}_x = \widetilde{b}_x[n]\ w_d[n] \ \overset{FT}{\longleftrightarrow}\ X(f) = \widetilde{X}(e^{j2\pi f_n}) \circledast W_d(e^{j2\pi f_n}) \tag{3.48}$$

where the periodically extended OFDM signal is time-limited with the T_s-sampled rectangular window $w_d(nT_s) = w_d[n]$ of duration $T = NT_s$, shown in figure 3.12(a). The FT of this discrete window is in turn given by

$$W_d(e^{j\omega}) = \frac{\sin(N\omega/2)}{\sin(\omega/2)} e^{-j\omega\frac{(N-1)}{2}} \tag{3.49}$$

which is a continuous and periodic spectrum with a period of 2π with respect to the normalized frecuency ω. Therefore, the FT in (3.46) will correspond to a *continuous* and *periodic* spectrum, equivalent to the superposition of an infinite number of replica of the OFDM base-band spectrum (N subcarriers) in shifted placements, each separated by the sampling frequency. An example of this is shown in figure 3.13 for a discrete window with length $2N$ and using twice the critical sampling rate.

As shown in figure 3.12(b), the discrete window spectrum can be discretized by taking frequency samples at the critical rate $\omega_k = \frac{2\pi k}{N}$ with $|k| = \{0, 1, 2, \ldots\}$, whence we obtain a discrete linear spectrum that presents null values except for the frequencies $|\omega_k| = \{0, 2\pi, 4\pi, \ldots\}$. This sampled version of the discrete window spectrum in (3.49) can also be expressed using the corresponding DFT,

$$W_d[k] = \frac{\sin(\pi k)}{\sin(\pi k/N)} e^{-j\pi k\frac{(N-1)}{N}}. \tag{3.50}$$

The extended discrete window and its corresponding spectrum are also shown in figure 3.12 for an extended length $N_1 = N + N_{CE}$, where for simplicity we choose $N = 10$ and $N_{CE} = 2$. Then, an extended window $w_1[n]$, of duration N_1, is applied over the virtual periodic sequence $\widetilde{b}_x[n]$ (see figure 3.11) to extract the extended symbol

$$\overline{\mathbf{b}}_x = \widetilde{b}_x[n]\ w_1[n].$$

Thence, the spectrum of the CE OFDM symbol shown in figure 3.11(a) could be obtained as,

$$\overline{X}(e^{j\omega}) = \widetilde{X}(e^{j\omega}) \circledast W_1(e^{j\omega}) = \frac{1}{2\pi}\int_{-\pi}^{\pi} \widetilde{X}(e^{j\omega'})W_1(e^{j(\omega-\omega')})d\omega' \tag{3.51}$$

where $\circledast$ denotes a circular convolution and $\widetilde{X}(e^{j\omega})$ is the FT (periodic) of $\widetilde{b}_x[n]$. Although the CE of an OFDM symbol, as described in previous sections, does not constitute by definition a periodic extension, the samples of the CE can be considered as a part of it. Thus, any N consecutive samples within the extended symbol $\overline{\mathbf{b}}_x$ could be considered as one periodic block extracted from the virtual periodic base-band signal shown in figure 3.11(b). Similarly, to define $\widetilde{b}_x[n]$ from the sequence $\mathbf{b}_x$ of length N, we define a periodical extension of this latter according to,

$$\widetilde{b}_x[n] = \sum_{m=-\infty}^{+\infty} b_x[n-mN] = b_x[n] \ * \sum_{m=-\infty}^{+\infty} \delta[n-mN] \tag{3.52}$$

so that $\widetilde{b}_x[n] = \widetilde{b}_x[n \pm mN]$ for any $\pm m$ integer. Note that the train of discrete-time deltas included in (3.52) corresponds to the following definition:

$$t[n] = \sum_{m=-\infty}^{+\infty} \delta[n-mN] = \begin{cases} 1 & ; \quad n = mN \\ 0 & ; \quad \text{otherwise.} \end{cases} \tag{3.53}$$

whose respective FT $\mathcal{F}(t[n])$ can be alternatively expressed by

$$T_\delta(e^{j2\pi f_n}) = \frac{1}{N}\sum_{k=-\infty}^{+\infty} \delta(f_n - \frac{k}{N}) = \frac{2\pi}{N}\sum_{k=-\infty}^{+\infty} \delta(\omega - 2\pi\frac{k}{N}) = \frac{1}{T}\sum_{k=-\infty}^{+\infty} \delta(f_n f_s - \frac{k}{T}). \tag{3.54}$$

Thus, with the PE defined through the convolution in (3.52), $\mathbf{b}_x$ becomes the sampled periodic signal $\widetilde{b}_x[n]$ whose corresponding spectrum

$$\begin{aligned} \widetilde{X}(e^{j\omega}) &= \sum_{n=-\infty}^{\infty} \widetilde{b}_x[n]e^{-jn\omega} = X(e^{j\omega})T_\delta(e^{j\omega}) \\ &= X(e^{j2\pi f_n})\frac{1}{N}\sum_{k=-\infty}^{+\infty} \delta(f_n - \frac{k}{N}) = X(e^{j2\pi\frac{f}{f_s}})\frac{1}{N}\sum_{k=-\infty}^{+\infty} \delta(\frac{f}{f_s} - \frac{k}{N}) \end{aligned} \tag{3.55}$$

is clearly periodic and discrete. Therefore, the FT of the CE symbol, $\overline{X}(e^{j\omega})$, can be completely characterized over the interval $\omega = [0, 2\pi]$ in discrete frequency domain by

suitably defining the DFT $X[k]$ of N samples from one period of the signal. The discrete equivalent for the spectrum in (3.55) is then

$$\widetilde{X}(e^{j\omega}) = \frac{2\pi}{\sqrt{N}} \sum_{k=-\infty}^{+\infty} X[k]\delta(\omega - 2\pi\frac{k}{N}) \tag{3.56}$$

where

$$X[k] = \frac{1}{\sqrt{N}} \sum_{n=0}^{N-1} b_x[n] e^{-j2\pi\frac{k}{N}n} \tag{3.57}$$

are the coefficients obtained with the DFT of the signal $\mathbf{b}_x$, associated to the unitary area analog deltas of its harmonic composition.

Then, given the discrete periodicity of the spectrum in (3.56) we can reevaluate (3.51) obtaining

$$\begin{aligned} \overline{X}(e^{j\omega}) &= \widetilde{X}(e^{j\omega}) \circledast W_1(e^{j\omega}) \\ &= \frac{2\pi}{\sqrt{N}} \sum_{k=-\infty}^{+\infty} X[k]\delta(\omega - 2\pi\frac{k}{N}) \circledast W_1(e^{j\omega}) \\ &= \frac{2\pi}{\sqrt{N}} \sum_{k=-\infty}^{+\infty} X[k] W_1(e^{j(\omega - 2\pi\frac{k}{N})}). \end{aligned} \tag{3.58}$$

The spectrum in (3.58) can be sampled in frequency at, say, $\omega_{k_0} = 2\pi\frac{k_0}{N}$, thus we can rewrite (3.58) as

$$\overline{X}(e^{j\omega_{k_0}})\big|_{\omega_{k_0}=2\pi\frac{k_0}{N}} = \frac{2\pi}{\sqrt{N}} \sum_{k=-\infty}^{+\infty} X[k] W_1(e^{j(\omega_{k_0} - 2\pi\frac{k}{N})}). \tag{3.59}$$

In this last expression we must observe that the condition

$$W_1(e^{j(\omega_{k_0} - 2\pi\frac{k}{N})}) = 0 \,; k_0 \neq k$$

is not always true if $N_1 > N$. It follows from this that the observed spectral values for each $\omega_{k_0} = 2\pi\frac{k_0}{N}$ will contain the data $X[k_0]$ of the corresponding sampled subcarrier, but additionally will present the ICI from the tails of the remaining subcarriers because they are no longer orthogonal as long as an extended length $N_1 > N$ has been applied for windowing. A simplified graphical example of this effect is shown in figure 3.14 for two adjacent subcarriers.

The ICI appearance described previously is just one of the critical aspects concerning the formulation of our discrete model. Basically, before introducing or testing any nonlinear block (HPA and linearization devices) we expect to provide a complete and accurate

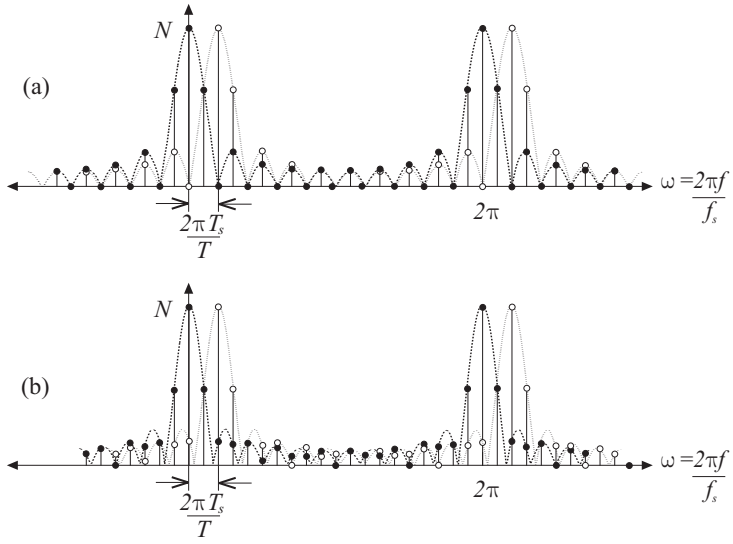

Figure 3.14: Sampled spectra at $w_{k_0} = k_o \frac{\pi T_s}{T}$ for two adjacent subcarriers (a) using an N-lenght discrete window (b) using the CE discrete window of lenght $N + N_{CP}$.

discrete model of a completely linear transmission chain. To achieve this, several important details with regard to the D/A conversion and signal propagation aspects must be carefully reviewed.

Note that from (3.47), in a normalized spectrum, the frequency allocation for the group of deltas that represent the N subcarriers of the base-band OFDM signal in (3.21) will be in general given by $\omega_k = 2\pi k \frac{T_s}{T}$, with $k = \{0, \ldots, N-1\}$. Thus, if the critical sampling rate $f_s = N/T$ is considered, the N subcarriers will be centered at $\omega_k = \frac{2\pi k}{N}$ which means that the N subcarriers will span the entire normalized frequency range $[0, 2\pi]$. Thus, according to the samlping theorem, the minimum sampling rate must be twice the bandwidth occupied by the N subcarriers of the OFDM signal, this is the Nyquist sampling rate given by $f_s = \frac{2N}{T}$.

3.3.3 D/A Conversion

In figure 3.15 two parallel chains are presented in a descriptive scheme where the left-hand branch is concerned with the transmission process of the virtual periodic signal $\widetilde{b}_x[n]$ while the right-hand branch represents the equivalent process for the real extended symbol $\overline{\mathbf{b}}_x$.

At the virtual branch, the D/A converter model can be conveniently split into two parts. First, a delta functions generator (DG) with a sampling frequency matching the ratio of the incoming sample stream $f_s = 1/T_s$ is applied. The analog impulses are weighted with each sample of the signal so that the signal at the output of the DG (marked with

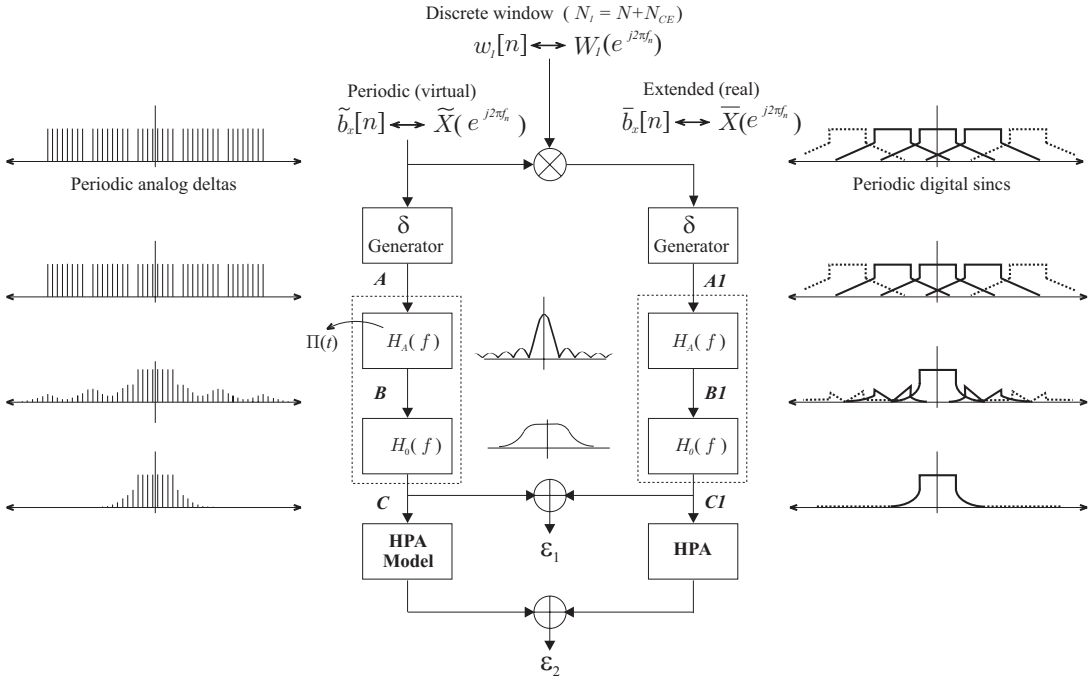

Figure 3.15: Equivalent transmission chains.

A in the figure) is expressed as

$$\widetilde{b}_x^A(t) = \sum_{m=-\infty}^{+\infty} \widetilde{b}_x[m]\delta(t - mT_s) \tag{3.60}$$

which is now an analog periodic signal whose FT is also periodic and can be expressed as

$$\widetilde{X}^A(f) = \widetilde{X}(f) * \frac{1}{T_s} \sum_{m=-\infty}^{+\infty} \delta(f - mf_s). \tag{3.61}$$

This device is then followed by a filter with rectangular (time-limited) impulse response of duration T_s that acts as a zero-order hold for each sample. Centered at the origin, the holding pulse is defined by

$$\Pi_{T_s}(t) = \begin{cases} 1 & ; \quad -\frac{T_s}{2} \leq t < \frac{T_s}{2} \\ 0 & ; \quad \text{otherwise} \end{cases} \tag{3.62}$$

whose corresponding spectrum is

$$P_{T_s}(f) = T_s \frac{\sin(\pi f T_s)}{\pi f T_s} = T_s \text{sinc}(f T_s). \tag{3.63}$$

The position of the delta function associated to each sample must coincide with the rising flank of its corresponding holding pulse. Therefore, the shifted pulse $\Pi_{T_s}\left(t - \frac{T_s}{2}\right)$ will

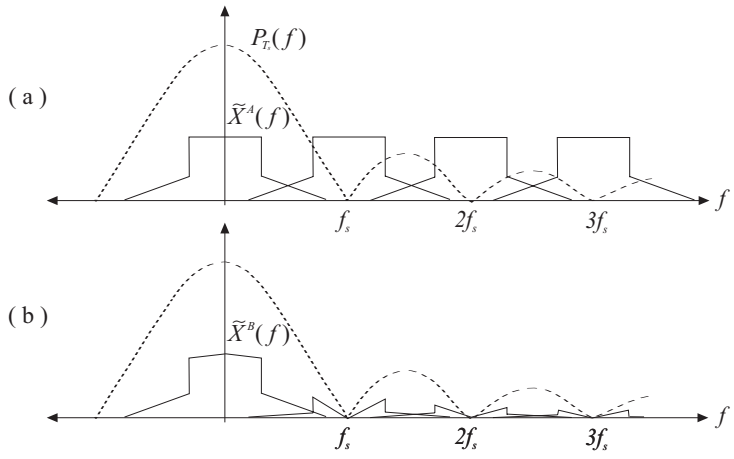

Figure 3.16: (a) Periodic spectrum at the output of the delta functions generator (b) the spectrum is no longer periodic after filtering with $P_{T_s}(f)$

be applied in combination with the weighted train of deltas from (3.60), thus producing an output at point B equal to

$$\widetilde{b}_x^B(t) = \Pi_{T_s}\Big(t - \frac{T_s}{2}\Big) * \widetilde{b}_x^A(t) \tag{3.64}$$

$$= \sum_{m=-\infty}^{+\infty} \widetilde{b}_x[m]\Pi_{T_s}\Big(t - \frac{T_s}{2} - mT_s\Big). \tag{3.65}$$

The frequency domain equivalent for $\widetilde{b}_x^B(t)$ can be obtained through the convolution between the spectrum of the first holding pulse, which is centered at $t = T_s/2$, and the periodic spectrum given in (3.61). This results in a non-periodic spectrum, as shown in figure 3.16, that can be calculated using (3.61) and (3.63) as follows:

$$\widetilde{X}^B(f) = \widetilde{X}^A(f)P_{T_s}(f)e^{-j2\pi f\frac{T_s}{2}} \tag{3.66}$$

where the phase shifting factor corresponds to a $T_s/2$ time shifting of the holding pulse.

After the sample and hold stages, the signal must be lowpass filtered with the reconstruction filter $H_0(f)$ before the HPA. At this point, it is a desirable condition, in light of the nonlinear distortion model presented in section 3.2.2, that the output spectrum of $H_0(f)$ be a general linear combination of orthogonal 'sinc' functions. This is because the multiconvolution of such functions becomes a single 'sinc' which could yield important simplifications for the formulation of the final analytical model.

Nature of $H_0(f)$

In general, there exist two different options to define the reconstruction filter. On one hand we could consider the 'bandlimited approach'. This is done by letting the frequency

profile of $H_0(f)$ be an ideal rectangular function presenting an infinite duration impulse response $h_0(t)$. On the other hand, we have the 'limited time' approach, where the impulse response of the filter $h_0(t)$ is considered time-limited to a duration D_H. Thus, the frequency equivalent of the filter can be expressed as a combination of 'sinc' functions which is suitable for modeling purposes.

The bandlimited approach can be characterized, for instance, by a Whittacker reconstruction procedure [53] where, according to the sampling theorem, a lowpass square filter with the transfer function

$$H_w(f) = \begin{cases} T & ; \quad -\frac{\pi}{T} \leq 2\pi f \leq \frac{\pi}{T} \\ 0 & ; \quad \text{otherwise} \end{cases}$$

is defined to reconstruct the signal $x(t)$ from a set of N samples $x[n]$. In this expression $1/T$ is the highest sampled signal frequency. Through this approach, the reconstructed version of the signal is obtained as

$$\widehat{x}(t) = \sum_{n=0}^{N-1} x[n] \frac{\sin[(\pi/T)(t-nT)]}{(\pi/T)(t-nT)}. \tag{3.67}$$

This sum in (3.67), called the Witthacker's cardinal function, is a general theoretic expression for reconstruction whose implementation is not possible due to the infinite duration of the components within the summation in (3.67). Besides this, a major disadvantage of the bandlimited filtering is that higher frequency components are completely eliminated. This is specially acute if we consider that much of the information of the pre-distorted signal will be contained in the tails of the regrown spectrum since the PD is a nonlinear operation.

Another example, this time for limited time filtering, can be the $H(s) = \frac{N(s)}{D(s)}$ filter structures given by a quotient of terms, in the Laplace transform domain, that determine the zeros/poles of the frequency response. When seen in time domain, the Laplace terms of such transfer functions become a combination of exponential terms (partial fraction expansions) that decrease quickly enough to be considered zero beyond a certain lapse of time. Butterworth filters are characterized by a smooth power gain characteristic which exhibit maximum flatness in the passband along with a cutoff transition whose sharpness depends on the number of poles of its transfer function.

Regarding these two possible approaches for the definition of the filter $H(f)$, a trade-off will arise between cutoff sharpness and the duration of the time impulse response of the filter. Then, the two main parameters involved are,

- D_x = Duration of the windowed symbol in time.

- D_h = Duration of the impulse response of the filter $H_0(f)$.

From equation (3.55) we know that $\widetilde{X}(f)$ is discrete and periodic. Then according to (3.61) the spectrum $\widetilde{X}^A(f)$ at the input of $H(f)$ is periodic and contains a combination of analog deltas instead of samples at $f = \frac{k}{NT_s}$. A general expression for the input of $H_0(f)$, at the point B, is given by,

$$\widetilde{X}^B(f) = \sum_{k=-\infty}^{+\infty} d_k \,\mathrm{sinc}\left[D_x(f - \frac{k}{D_x})\right] e^{jD_x\pi(f-\frac{k}{D_x})}.$$

While, in general, any filter with a time-limited impulse response $h_0(t)$ corresponds to an unlimited bandwidth frequency response that can be expressed in the form,

$$H_0(f) = \sum_{k'=-\infty}^{+\infty} H_{k'}\mathrm{sinc}\left[\frac{f - k'/D_h}{1/D_h}\right].$$

Hence, the filtering operation could be expressed as a linear combination of the resulting product of sincs,

$$\begin{aligned}\widetilde{Y}^C(f) &= \widetilde{X}^B(f)H_0(f) \\ &= \sum_{k=-\infty}^{+\infty}\sum_{k'=-\infty}^{+\infty} d_k H_{k'}\,\mathrm{sinc}\left[D_x(f - \frac{k}{D_x})\right]\mathrm{sinc}\left[\frac{f - k'/D_h}{1/D_h}\right] e^{jD_x\pi(f-\frac{k}{D_x})}\end{aligned}$$

which will likely lead us to intractable expressions without a closed form to decribe the input to the HPA.

Finally, it is noteworthy to mention that the D/A conversion process, performed along the left branch in figure 3.15, has the advantage that the resulting spectrum at A, B and C will contain only analog deltas since the blocks at every step deal with periodic signals. Therefore, filtering with $H_0(f)$ corresponds in this case to a simple area-scaling of the analog deltas that compose the spectrum at B according to the frequency mask of the filter. In contrast, the same filtering with $H_0(f)$ has more modeling complexities when it is carried out over the spectral components of the real extended signal at the right branch (continuous sincs). The sidelobe tails of a sinc frequency pattern, obtained as the FT of a rectangular pulse, present a slow decaying profile which may lead to high levels of intercarrier interference (ICI) and broadly affect the bandwidth of interest. If the frequency response of the filter is assumed to vary slowly with respect to the subcarrier bandwidth, then the filtering selectivity could be approximated as a constant gain for each component and we can consider simple component scaling for the model. However, when the filter gain varies significantly within the subchannel bandwidth, filtering forces the spectral components to loose its original symmetry so they can no longer be treated as sinc frequency patterns. This negative effect will be specially acute for modeling

purposes for the cases when the signal spectrum contains non-orthogonal sincs. Thence, modeling the transmission process for the real available sampled signal will require the formulation of an exact equivalent discrete model where the influence of any approximation or constraint in the sense of D/A compatibilities can be quantified and controlled.

3.4 Exact Equivalent Discrete Model for Transmission

In order to develop a reliable theoretical model for the precise assessment and correction of the nonlinear transference of an OFDM signal, we must reduce to a minimum the approximations carried out in the modeling of those system components not involved in the nonlinear distortion effect itself. This will allow us to quantify the ICI and other mismatching effects at the receiving end as well as at each stage within the chain independently from the inherent sources of impairment due to the structure of the OFDM system. Thus, the aim of this new section is the formulation of an exact equivalent discrete model for the transmission chain, including those stages we have been reviewing and the final reception of the signal, namely: IFFT modulation, cyclic prefix addition, digital to analog conversion, channel propagation effects, analog to digital conversion and, finally, FFT demodulation of the M-QAM information.

Under the single assumption of a time-limited impulse response channel, we aim to establish an end-to-end transmission model. Therefore, without loss of generality, the channel frequency response and the rectangular (zero-order hold) and reconstruction filters $H_0(f)$ defined for D/A conversion, can all be merged into a single frequency response $H(f)$.

According to the model previously presented in figure 3.15, we consider first the basic expression for the FT at the output of the delta generator:

$$\widetilde{X}^A(f) = \sum_{m=-\infty}^{+\infty} d_m \, \delta\left(f - \frac{m}{T}\right) \tag{3.68}$$

where d_m are the M-QAM data over the m-th subcarrier. After DG, d_m is a periodic sequence with $d_m = d_{m+kN}$, which is in accordance with the PE defined in (3.52) for N subcarriers as well.

As we have seen previously in section 3.2.1 for analog continuous OFDM signals, the use of the CE causes the subcarriers to lose orthogonality between them. Therefore, direct use of such signals will make more difficult the modeling of filtering operation with $H(f)$, whose main complexity in such a case is expressing the product of non-orthogonal sincs. The modeling solution is then shown in figure 3.17(d)[2] where a new periodic input $\widetilde{\overline{b}}_x$ is suitably defined considering the CE as well as the guard time T_G as part of a periodic block of duration $T_2 = T + T_{CE} + T_G$. The CE and the GT are chosen so that

[2]The schemes in the figure are valid to proportionally represent sample frames as well as continuous time signals.

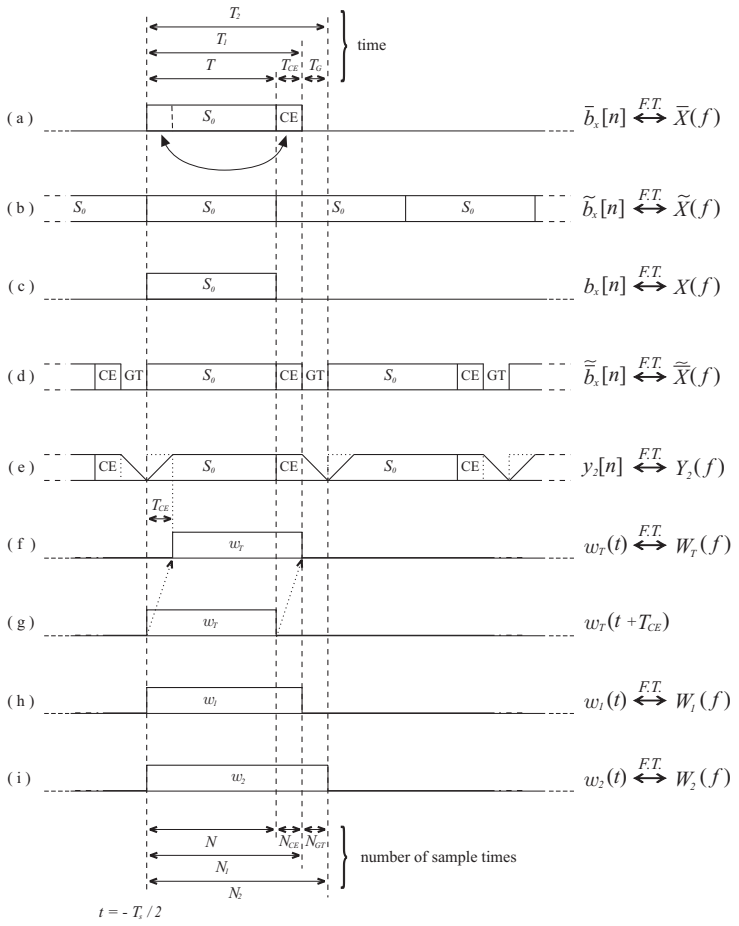

Figure 3.17: Time diagrams for different signal and windows defined for the model. Note that a $T_s/2$ time shift is defined between continuous signals/windows and their respective sampled versions in order to prevent any discontinuity to coincide with sample positions.

$T_G \geq T_{CE} \geq T_h$, with T_h being the duration of the channel impulse response. Then, in the figure, $T_2 = T + 2T_h$ is shown to be the minimum time window necessary to contain the CE OFDM symbol avoiding interference from neighbouring symbols. The new auxiliary signal is then defined as,

$$\begin{aligned} \widetilde{\overline{b}}_x &= \sum_{\ell=-\infty}^{+\infty} \overline{b}_x(t-\ell\,T_2)w_1(t-\ell\,T_2) \\ &= \sum_{\ell=-\infty}^{+\infty} \widetilde{b}_x(t-\ell\,T_2)w_1(t-\ell\,T_2) = \sum_{m_2=-\infty}^{+\infty} c_{m_2} e^{j2\pi\frac{m_2}{T_2}t} \end{aligned} \tag{3.69}$$

with $w_1(t) = \Pi_{T_1}\left(t - \frac{T_1}{2} + \frac{T_s}{2}\right)$ the rectangular window of duration $T_1 = T + T_{CE}$ (extended symbol duration), which is shown in figure 3.17(h). The Fourier series coefficients

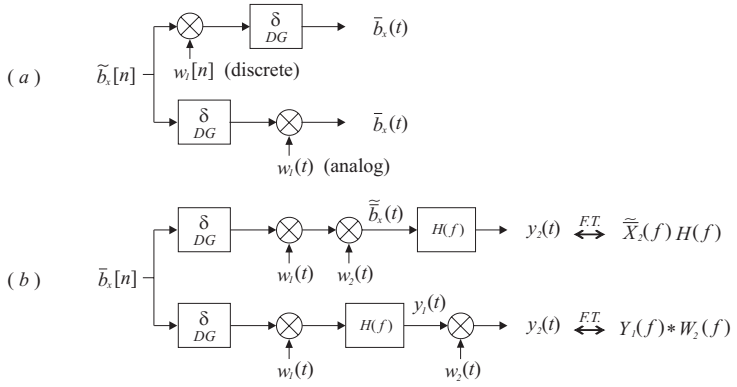

Figure 3.18: Equivalent windowing (a) to obtain the CE symbol (b) to express the filtered output.

c_{m_2}, included in (3.69), also define the corresponding FT of the auxiliary signal as follows:

$$\overline{\widetilde{X}}(f) = \sum_{m_2=-\infty}^{+\infty} c_{m_2}\delta\left(f - \frac{m_2}{T_2}\right). \tag{3.70}$$

For the calculation of the coefficients c_{m_2}, a basic signal block for (3.69) can be defined. Recalling the model in figure 3.15, such basic block is the signal at $A1$, that is, at the output of the DG on the left branch. Nevertheless, an equivalent signal could be obtained through the discrete-analog windowing equivalence shown in figure 3.18. Thence, windowing the analog periodic DG output $\widetilde{b}_x^A(t)$ with the one-symbol+CE long window $w_1(t)$, we have

$$\overline{b}_x(t) = \widetilde{b}_x^A(t)w_1(t) \quad \overset{FT}{\longleftrightarrow} \quad \overline{X}(f) = \widetilde{X}^A(f) * W_1(f) \tag{3.71}$$

where it is important to note that the components of the FT of this basic signal,

$$\overline{X}(f) = \sum_{m=-\infty}^{+\infty} d_m W_1\left(f - \frac{m}{T}\right), \tag{3.72}$$

are non-orthogonal sincs (section 3.2.1) given the extended duration of the window $w_1(t)$. Then, since the coefficients c_{m_2} of the Fourier Series expansion can be expressed in terms of the FT of the basic signal as

$$c_{m_2} = \frac{1}{T_2}\overline{X}\left(\frac{m_2}{T_2}\right) \tag{3.73}$$

we have, substituting in (3.72), the final discrete expression for the new information coefficients,

$$c_{m_2} = \frac{1}{T_2}\sum_{m=-\infty}^{+\infty} d_m W_1\left(\frac{m_2}{T_2} - \frac{m}{T}\right). \tag{3.74}$$

These coefficients are relevant since they will contain a combination of the original M-QAM symbols d_m that, given (3.74) and the FT of the time window, can be seen as the interpolation of such symbols in frequency by means of a set of sinc functions. At this point we can suppose the periodicity of the coefficients c_{m_2} which is demonstrated in later expressions.

From (3.70) and (3.74) we obtain

$$\widetilde{\overline{X}}(f) = \sum_{m_2=-\infty}^{+\infty} \left(\frac{1}{T_2} \sum_{m=-\infty}^{+\infty} d_m W_1 \left(\frac{m_2}{T_2} - \frac{m}{T} \right) \right) \delta \left(f - \frac{m_2}{T_2} \right). \tag{3.75}$$

Then, as shown in figure 3.17(h), along with the filtering with $H(f)$, an additional window w_2 of duration $T_2 = T + T_{CE} + T_G$ can be applied without modifying the signal structure defined in (3.69). In such case, the filter output $y_2(t)$ will also be limited in time to T_2 and admits two equivalent ways for its evaluation. In time domain this is given by

$$y_2(t) = \left(w_2(t) \widetilde{\overline{b}}_x(t) \right) * h(t) = \left(\widetilde{\overline{b}}_x(t) * h(t) \right) w_2(t) \tag{3.76}$$

and expressed in frequency domain

$$Y_2(f) = \left(W_2(f) * \widetilde{\overline{X}}(f) \right) H(f) = \widetilde{\overline{X}}_2(f) H(f) \tag{3.77}$$

$$= \left(\widetilde{\overline{X}}(f) H(f) \right) * W_2(f) = Y_1(f) * W_2(f). \tag{3.78}$$

These are the two alternative and equivalent ways to place the analog window $w_2(t)$ that we consider in figure 3.18(b). Then, in particular, the evaluation of (3.78) using (3.70) yields

$$Y_2(f) = \left(\sum_{m_2=-\infty}^{+\infty} \left[c_{m_2} H \left(\frac{m_2}{T_2} \right) \right] \delta \left(f - \frac{m_2}{T_2} \right) \right) * W_2(f) \tag{3.79}$$

$$= \sum_{m_2=-\infty}^{+\infty} g_{m_2} W_2 \left(f - \frac{m_2}{T_2} \right) \tag{3.80}$$

where we define $g_{m_2} = c_{m_2} H \left(\frac{m_2}{T_2} \right)$ as the coefficients to express the filter output on a new base, such that the set of windows $W_2 \left(f - \frac{m_2}{T_2} \right)$ associated to these coefficients is now an orthogonal pattern of sincs. The orthogonality between them make the components in (3.80) sufficient to precisely describe the spectrum $Y_2(f)$ at the input of the HPA, even if discarding any assumption on the variation of H(f) with respect to the subcarrier bandwidth. This latter requires that the frequency spectrum be sampled at least with a step $\Delta f = 1/T_2 < 1/T$.

It is important here to remark on the first relation between the originally transmitted M-QAM symbols d_m and the final coefficients g_{m_2}. Using (3.74), we can express

$$g_{m_2} = H\left(\frac{m_2}{T_2}\right)\frac{1}{T_2}\sum_{m=-\infty}^{+\infty} d_m W_1\left(\frac{m_2}{T_2}-\frac{m}{T}\right) \tag{3.81}$$

and, replacing in (3.80), $Y_2(f)$ in extension gives

$$Y_2(f) = \sum_{m_2=-\infty}^{+\infty} H\left(\frac{m_2}{T_2}\right)\frac{1}{T_2}\sum_{m=-\infty}^{+\infty} d_m W_1\left(\frac{m_2}{T_2}-\frac{m}{T}\right) W_2\left(f-\frac{m_2}{T_2}\right). \tag{3.82}$$

Let us now consider a perfectly linear transference of the signal, i.e., an ideal cancellation of the nonlinear effect of the HPA. In reception, the signal is windowed by $w_T(t)$ (figure3.17(f)) being expressed as

$$y_T(t) = y_2(t)w_T(t) \quad \overset{FT}{\longleftrightarrow} \quad Y_T(f) = Y_2(f) * W_T(f). \tag{3.83}$$

This windowing operation restores the orthogonality for the N original subcarriers and is assumed to be synchronous in order to avoid any intersymbol interference (ISI) from the time response associated to the filtering operation. This is shown in figure 3.17(e) and (f) for the critical case when the total impulse response equals the guard time.

After sampling $y_T(t)$ with $f_s = \frac{N}{T}$, we have a periodic spectrum $Y_T(e^{j2\pi f_n}) = \widetilde{Y}(f_n)$ that can be expressed applying the sampling theorem as

$$Y_T(e^{j2\pi f_n}) = \widetilde{Y}(f_n) = \frac{1}{T_s}\sum_{k=-\infty}^{+\infty} Y_T\big(f-kf_s\big) = \frac{1}{T_s}\sum_{k=-\infty}^{+\infty} Y_T\big((f_n-k)f_s\big) \tag{3.84}$$

with $f_n = \frac{f}{f_s}$ the normalized frequency. This equivalence can be further developed resorting to the specific formulation of the sampling theorem shown in the appendix (3.A) for analog and discrete sincs. Therein we show that

$$\boxed{\widetilde{W}(f_n) = \frac{1}{T_s}\sum_{m=-\infty}^{+\infty} W\big((f_n-m)f_s\big)} \tag{3.85}$$

where $\widetilde{W}(f_n)$ is the FT of the sampled version of a continuous equivalent rectangular window whose FT is in turn $W(f)$. Then, from (3.83) and (3.80) we obtain,

$$Y_T(f) = \sum_{m_2=-\infty}^{+\infty} g_{m_2} W_2\left(f-\frac{m_2}{T_2}\right) * W_T(f) = \sum_{m_2=-\infty}^{+\infty} g_{m_2} W_T\left(f-\frac{m_2}{T_2}\right)$$

and using (3.84),

$$\begin{aligned}
\widetilde{Y}_T(f_n) &= \frac{1}{T_s}\sum_{k=-\infty}^{+\infty}\sum_{m_2=-\infty}^{+\infty} g_{m_2} W_T\left((f_n-k)\frac{N}{T}-\frac{m_2}{T_2}\right) \\
&= \frac{1}{T_s}\sum_{m_2=-\infty}^{+\infty} g_{m_2}\sum_{k=-\infty}^{+\infty} W_T\left((f_n-k)\frac{N}{T}-\frac{m_2}{T_2}\right) \\
&= \frac{1}{T_s}\sum_{m_2=-\infty}^{+\infty} g_{m_2}\sum_{k=-\infty}^{+\infty} W_T\left[\left(\left(f_n-\frac{T}{T_2}\frac{m_2}{N}\right)-k\right)\frac{N}{T}\right] \\
&= \sum_{m_2=-\infty}^{+\infty} g_{m_2}\widetilde{W}_T\left(f_n-\frac{T}{T_2}\frac{m_2}{N}\right) \qquad (3.86)
\end{aligned}$$

where $\widetilde{W}_T$ corresponds to a discrete periodic equivalent spectrum for the sampled version [3] of $w_T(t)$. Let us now introduce a hypothesis of periodicity that can be useful to express (3.86) in a more compact form containing only finite summations. This is done by using the index $m_2 = m_2' + N_2 m_2''$ with $0 \le m_2' \le (N_2-1)$ and $-\infty < m_2'' < +\infty$. Then (3.86) becomes

$$\widetilde{Y}_T(f_n) = \sum_{m_2'=0}^{N_2-1}\sum_{m_2''=-\infty}^{+\infty} g_{m_2'+N_2m_2''}\widetilde{W}_T\left(f_n-\frac{T}{T_2}\left(\frac{m_2'+N_2m_2''}{N}\right)\right)$$

and since $\frac{N}{T}=\frac{N_2}{T_2}$, with $\widetilde{W}_T$ periodic with period 1 in f_n, we have

$$\widetilde{Y}_T(f_n) = \sum_{m_2'=0}^{N_2-1}\Bigg[\underbrace{\sum_{m_2''=-\infty}^{+\infty} g_{m_2'+N_2m_2''}}_{\gamma_{m_2'}}\Bigg]\widetilde{W}_T\left(f_n-\frac{T}{T_2}\frac{m_2'}{N}\right). \qquad (3.87)$$

In this last expression we define,

$$\gamma_{m_2'} = \sum_{m_2''=-\infty}^{+\infty} g_{m_2'+N_2m_2''}$$

and substituting $g_{m_2} = c_{m_2}H\left(\frac{m_2}{T_2}\right)$ we obtain,

$$\gamma_{m_2'} = \sum_{m_2''=-\infty}^{+\infty} c_{m_2'+N_2m_2''}H\left(\frac{m_2'+N_2m_2''}{T_2}\right). \qquad (3.88)$$

Now, introducing the periodicity for the index $m = m' + Nm''$, with $0 \le m' \le (N-1)$ and $-\infty < m'' < +\infty$, we can re-express $c_{m_2'+N_2m_2''}$ from (3.74) as

[3] In figure 3.17 the samples are defined so that they do not coincide with discontinuities at the extremes of rectangular windows.

$$c_{m_2'+N_2m_2''} = \frac{1}{T_2}\sum_{m'=0}^{N-1}\sum_{m''=-\infty}^{+\infty} d_{m'+Nm''} W_1\left(\frac{m_2'+N_2m_2''}{T_2} - \frac{m'+Nm''}{T}\right) \tag{3.89}$$

and since $d_{m'} = d_{m'+Nm''}$ with the sampling frequency given by $f_s = \frac{N}{T} = \frac{N_2}{T_2}$, we can write

$$\begin{aligned} c_{m_2'+N_2m_2''} &= \frac{1}{T_2}\sum_{m'=0}^{N-1} d_{m'} \sum_{m''=-\infty}^{+\infty} W_1\left((m_2''-m'')f_s + \frac{m_2'}{T_2} - \frac{m'}{T}\right) \\ &= \frac{1}{T_2}\sum_{m'=0}^{N-1} d_{m'} \sum_{m''=-\infty}^{+\infty} W_1\left(\left(\frac{m_2'}{N_2} - \frac{m'}{N} + m_2'' - m''\right)f_s\right) \\ &= \frac{T_s}{T_2}\sum_{m'=0}^{N-1} d_{m'}\widetilde{W}_1\left(\frac{m_2'}{N_2} - \frac{m'}{N}\right) = c_{m_2'} \end{aligned} \tag{3.90}$$

which is the demonstration of the periodicity of c_{m_2}. Using this last result, and with the sampling frequency given by $f_s = \frac{N_2}{T_2}$, the expression for the coefficients in (3.88) can be reduced to

$$\begin{aligned} \gamma_{m_2'} &= c_{m_2'} \sum_{m_2''=-\infty}^{+\infty} H\left(\frac{m_2'+N_2m_2''}{T_2}\right) = c_{m_2'}\widetilde{H}\left(\frac{m_2'}{T_2}\right) \\ &= c_{m_2'} \sum_{m_2''=-\infty}^{+\infty} H\left[\left(\frac{m_2'}{N_2} + m_2''\right)f_s\right] = c_{m_2'}T_s\widetilde{H}\left(\frac{m_2'}{N_2}\right) \end{aligned} \tag{3.91}$$

where now $\widetilde{H}\left(\frac{m_2'}{N_2}\right)$ corresponds to samples (in normalized frequency) of a periodic spectrum defined from the periodic extension of the time-limited impulse response $h(t)$. In figure 3.19 the periodic extension of $h(t)$, obtained through the convolution $h(t) * \sum_{m=-\infty}^{+\infty}\delta(t-mT_2)$, is then sampled with $f_s = \frac{1}{T_s} = \frac{N_2}{T_2}$. This gives the periodic discrete spectrum depicted in figure 3.19(D) which is equivalent to sampling the continuous and periodic FT of $h[n]$ at $f_n = \frac{m_2'}{N_2}$ with m_2' integer. Then, resuming the expression for $\widetilde{Y}_T(f_n)$ we replace this last result in (3.87) using also (3.90) and obtaining

$$\widetilde{Y}_T(f_n) = \sum_{m_2'=0}^{N_2-1}\left(\frac{T_s^2}{T_2}\widetilde{H}\left(\frac{m_2'}{N_2}\right)\sum_{m'=0}^{N-1} d_{m'}\widetilde{W}_1\left(\frac{m_2'}{N_2} - \frac{m'}{N}\right)\right)\widetilde{W}_T\left(f_n - \frac{T}{T_2}\frac{m_2'}{N}\right). \tag{3.92}$$

Then, from the properties of the DFT expressed in appendix 3.B we know that

$$\widetilde{Y}_T(f_n) = \sum_{k=0}^{N-1} Y_T[k]\widetilde{W}_T\left(f_n - \frac{k}{N}\right) \tag{3.93}$$

$$Y_T[k] = Y_T(e^{j2\pi k/N}) = e^{j2\pi T_{CE}k/T}Y_N[k] \tag{3.94}$$

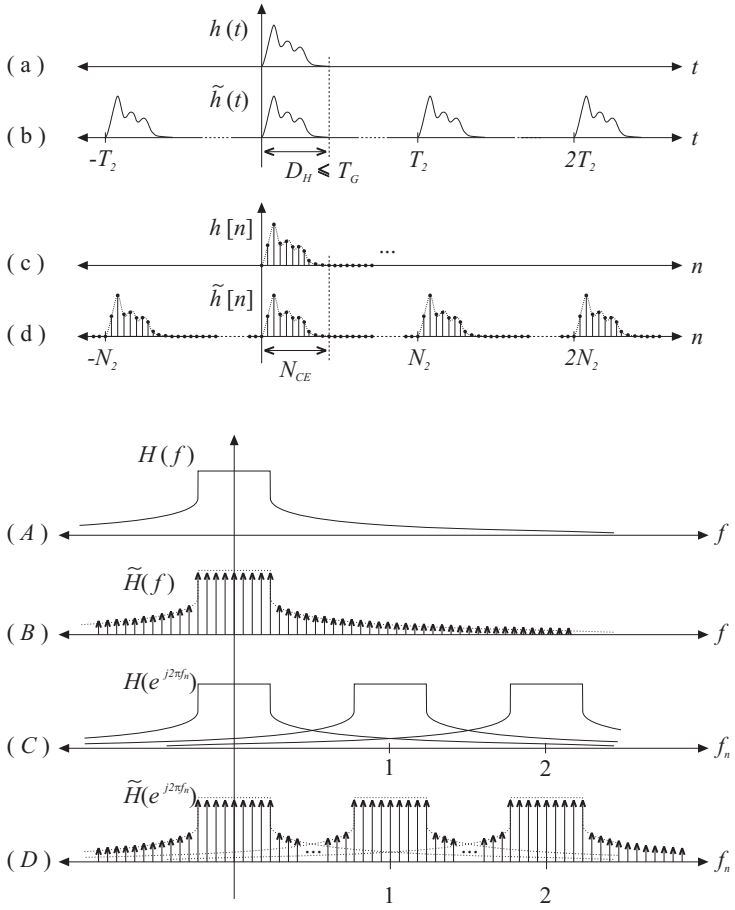

Figure 3.19: Time–frequency definitions based on the impulse response of the filter $h(t)$

which is convenient to find a discrete version of $\widetilde{Y}_T(f_n)$. However, (3.92) has the inconvenience that a non-integer shift is defined for $\widetilde{W}_T(\cdot)$ since $\frac{T}{T_2}\frac{m_2'}{N} \neq \frac{k}{N}$. This nuisance can be circumvented by applying the following property valid for the discrete window (see appendix 3.C again):

$$\widetilde{W}_T\left(\frac{p-r}{N}\right) = \sum_{q=0}^{N-1} \beta_r(q)\widetilde{W}_T\left(\frac{p-q}{N}\right) \tag{3.95}$$

whereby, with q integer, the fractional shift $r = \frac{T}{T_2}m_2'$ is sinthetized as a linear combination of N integer shifted versions of the same window in frequency domain. Thus, using this equivalency and substituting $N_2 = T_2/T_s$ in (3.92) we obtain

$$\begin{aligned} Y_T(e^{j2\pi\frac{p}{N}}) &= \sum_{m_2'=0}^{N_2-1}\left(\frac{T_s}{N_2}\widetilde{H}\left(\frac{m_2'}{N_2}\right)\sum_{m'=0}^{N-1}d_{m'}\widetilde{W}_1\left(\frac{m_2'}{N_2}-\frac{m'}{N}\right)\right)\sum_{q=0}^{N-1}\beta_{\frac{T}{T_2}m_2'}(q)\widetilde{W}_T\left(\frac{p-q}{N}\right) \\ &= \sum_{q=0}^{N-1}b_q\widetilde{W}_T\left(\frac{p-q}{N}\right) \end{aligned} \tag{3.96}$$

where the set of b_q will represent the demodulated M-QAM symbols at the receiver. Each component b_q seen through the DFT property given in (3.93) is expressed as

$$\begin{aligned} b_q &= \sum_{m_2'=0}^{N_2-1}\beta_{\frac{T}{T_2}m_2'}(q)\left(\frac{T_s}{N_2}\widetilde{H}\left(\frac{m_2'}{N_2}\right)\sum_{m'=0}^{N-1}d_{m'}\widetilde{W}_1\left(\frac{m_2'}{N_2}-\frac{m'}{N}\right)\right) \\ &= \frac{T_s}{N_2}\sum_{m'=0}^{N-1}d_{m'}\sum_{m_2'=0}^{N_2-1}\beta_{\frac{T}{T_2}m_2'}(q)\widetilde{H}\left(\frac{m_2'}{N_2}\right)\widetilde{W}_1\left(\frac{m_2'}{N_2}-\frac{m'}{N}\right). \end{aligned} \tag{3.97}$$

Then, using $\frac{T}{T_2}=\frac{N}{N_2}$ in the expression for $\beta_r(q)$ obtained in appendix 3.B, we replace

$$\beta_{\frac{T}{T_2}m_2'}(q)=\beta_r(q)=\frac{1}{N}\widetilde{W}_T\left(\frac{q-r}{N}\right)=\frac{1}{N}\widetilde{W}_T\left(\frac{q}{N}-\frac{m_2'}{N_2}\right)$$

in (3.97) and finally obtain

$$b_q=\frac{T_s}{N\cdot N_2}\sum_{m'=0}^{N-1}d_{m'}\sum_{m_2'=0}^{N_2-1}\widetilde{H}\left(\frac{m_2'}{N_2}\right)\widetilde{W}_T\left(\frac{q}{N}-\frac{m_2'}{N_2}\right)\widetilde{W}_1\left(\frac{m_2'}{N_2}-\frac{m'}{N}\right). \tag{3.98}$$

This final equation can be expressed in vectorial notation as

$$\mathbf{b}_y=\mathbf{S}\mathbf{d}_x=\sum_{m'=0}^{N-1}d_{m'}\mathbf{s}_{m'} \tag{3.99}$$

where the matrix $\mathbf{S}$ is a $(N\times N)$ square matrix wherein the column vectors $\mathbf{s}_{m'}$ represent the contribution of each symbol $d_{m'}$ to each of the N demodulated subcarriers at the receiver. The elements of $\mathbf{S}$ are given by

$$\boxed{[\mathbf{S}]_{q,m'}=\frac{T_s}{N\cdot N_2}\sum_{m_2'=0}^{N_2-1}\widetilde{H}\left(\frac{m_2'}{N_2}\right)\widetilde{W}_T\left(\frac{q}{N}-\frac{m_2'}{N_2}\right)\widetilde{W}_1\left(\frac{m_2'}{N_2}-\frac{m'}{N}\right)}. \tag{3.100}$$

In the appendix 3.C we show that $\mathbf{S}$ is a diagonal matrix. The N elements of the main diagonal are given by

$$[\mathbf{S}]_{m'=q} = \frac{T_s}{N}\widetilde{z}[0] \mid_{m'=q} = T_s H[m']. \tag{3.101}$$

These elements can be seen as the DFT values of a periodic extension (with period N) of the time-limited impulse response $h[n]$ given by

$$\widetilde{h}_N[n] = h[n] * \sum_{m=-\infty}^{+\infty} \delta[n + Nm]$$

where,

$$\widetilde{h}_N[n] = 0 \; ; \text{ for } kN + N_{CE} \leq n < kN - 1.$$

Let us consider the limited duration of $h(t)$, denoted T_c, as the coherence time that respectively defines a coherence bandwidth $B_c = \frac{1}{T_c}$ which leads to a minimum set of coefficients sufficient to describe the frequency response of the filter. We define the minimum-distance non-overlapping periodic extension $\overline{h}_{T_c}(t)$ and its Fourier transform, both shown in figure 3.20(b) and (B) respectively, as follows:

$$\overline{h}_{T_c}(t) = h(t) * \sum_{m=-\infty}^{+\infty} \delta(f - mT_c) \overset{FT}{\longleftrightarrow} \overline{H}_{T_c}(f) = \sum_{q=-\infty}^{+\infty} B_q \delta(f - \frac{q}{T_c})$$

where B_q are the areas for the infinite spectral components (analog deltas) of the non periodic spectrum $\overline{H}_{T_c}(f)$. Note that, since the coherence bandwidth is being considered, this spectrum is described with a minimum number of maximum spaced spectral components. Then, if we apply a unitary window $w_{T_c}(t)$ of duration T_c over the first period of $\overline{h}_{T_c}(t)$, we have

$$h(t) = w_{T_c}(t)\overline{h}_{T_c}(t) \overset{FT}{\longleftrightarrow} H(f) = W_{T_c}(f) * \overline{H}_{T_c}(f) = \sum_{q=-\infty}^{+\infty} B_q W_{T_c}(f - \frac{q}{T_c})$$

where,

$$W_{T_c}(f) = T_c \frac{\sin(\pi T_c f)}{\pi T_c f} e^{-j\pi(T_c - T_s)f}$$

is the FT of the continuous window $w_{T_c}(t)$ which considers the $T_s/2$ shifting to avoid discontinuities at the sample positions. Then, according to the sampling theorem, we can construct the periodic spectrum of the equivalent sampled signal $h[n]$ as

$$H(e^{j2\pi f_n}) = \sum_{n=0}^{N-1} h[n] e^{-j2\pi f_n n} = \frac{1}{T_s} \sum_{k=-\infty}^{+\infty} H\left((f_n - k) f_s\right)$$

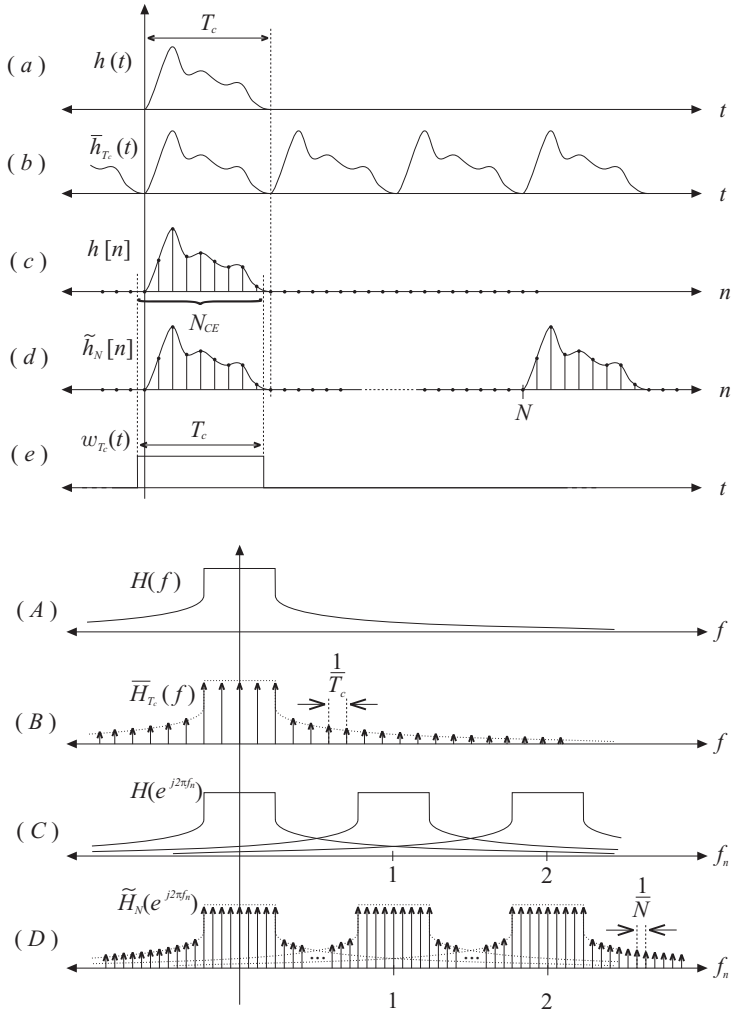

Figure 3.20: Time-frequency definitions used to define a minimum set of N_{CE} coefficients to identify the time-limited impulse response filter $H(f)$, based on the coherence bandwidth B_c.

with $T_s = \frac{T_c}{N_{CE}}$ and N_{CE} the number of samples available for $h[n]$. Then, replacing $H(f)$ and considering samples at $f_n = \frac{m}{N}$ we have

$$\begin{aligned}
H[m] &= \sum_{n=0}^{N-1} h[n] e^{-j2\pi \frac{m}{N} n} = \frac{N_{CE}}{T_c} \sum_{k=-\infty}^{+\infty} \sum_{q=-\infty}^{+\infty} B_q W_{T_c} \left((\frac{m}{N} - k) \frac{N_{CE}}{T_c} - \frac{q}{T_c} \right) \\
&= \frac{N_{CE}}{T_c} \sum_{q=-\infty}^{+\infty} B_q \sum_{k=-\infty}^{+\infty} W_{T_c} \left((\frac{m}{N} - k) \frac{N_{CE}}{T_c} - \frac{q}{T_c} \right) \\
&= \frac{N_{CE}}{T_c} \sum_{q=-\infty}^{+\infty} B_q \sum_{k=-\infty}^{+\infty} W_{T_c} \left((\frac{m}{N} - \frac{q}{N_{CE}} - k) \frac{N_{CE}}{T_c} \right) \\
&= \sum_{q=-\infty}^{+\infty} B_q \widetilde{W}_{T_c} \left(\frac{m}{N} - \frac{q}{N_{CE}} \right)
\end{aligned} \tag{3.102}$$

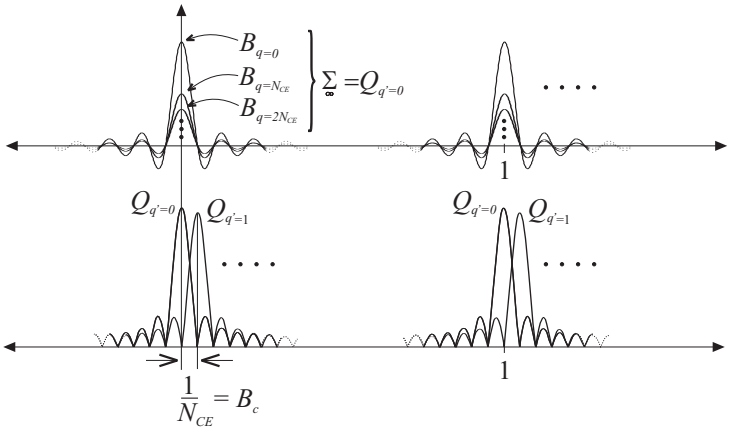

Figure 3.21: Composition of the final set of discrete sincs and its related N_{CE} coefficients $Q_{q'}$. The DFT values $H[m]$ are interpolated at the frecuencies $f_n = \frac{m}{N}$, with $m = \{0, 1, 2, \ldots, N-1\}$.

where the sampling theorem has been applied to replace $\widetilde{W}_{T_c}(f_n)$, the corresponding FT for the sampled version of $w_{T_c}(t)$. The summation of these periodic spectrums for the infinite values of B_q finally leads to a new (limited) set of coefficients $Q_{q'}$ which present a periodicity with respect to the new index q'. This is represented in figure 3.21 and allows us to express (3.102) with the following limited summation:

$$H[m] = \sum_{q'=0}^{N_{CE}-1} Q_{q'} \widetilde{W}_{T_c}\left(\frac{m}{N} - \frac{q'}{N_{CE}}\right). \tag{3.103}$$

From this last expression we can conclude that, given the coherence bandwidth $B_c = \frac{1}{T_c}$, the limited impulse response $h(t)$ can be expressed with a minimum set of N_{CE} coefficients $Q_{q'}$, suitably defined using a sufficient sampling time $T_s = \frac{T_c}{N_{CE}}$.

3.A Appendix: Equivalence of discrete and analog 'sinc' functions for the representation of Power Spectral Densities

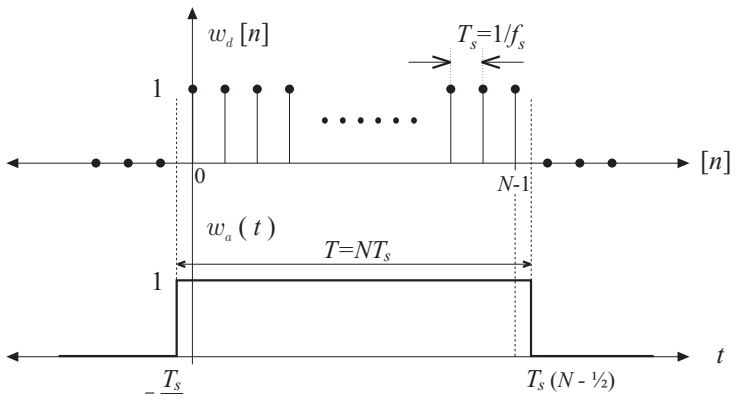

Figure 3.22: Equivalent functions for windowing.

This appendix includes a particular case for the application of the sampling theorem. It is shown how the spectrum resulting from taking the FT of a discrete pulse of length N, can be equivalently obtained through the infinite summation of analog "sinc" spectra that correspond to the FT of a continuous time window.

Let us consider first the continuous time unitary window $w(t)$ of duration $T = NT_s$, defined by

$$w_a(t) = \begin{cases} 1 & ; \quad -\frac{T_s}{2} \leq t < T - \frac{T_s}{2} \\ 0 & ; \quad \text{otherwise} \end{cases} \tag{3.104}$$

and then its equivalent discrete window

$$w_d[n] = \begin{cases} 1 & ; \quad 0 \leq n \leq N-1 \\ 0 & ; \quad \text{otherwise} \end{cases} \tag{3.105}$$

which is defined by taking N samples of (3.104) at the sampling frequency $f_s = 1/T_s$, so that $NT_s = T$. The samples are defined as to be taken at $t = nT_s$, as shown in figure 3.22.

The Fourier Transform for (3.104) is given by

$$W_a(f) = NT_s \text{sinc}(NT_s f) e^{-j2\pi \frac{(N-1)}{2} T_s f} = NT_s \frac{\sin(\pi NT_s f)}{(\pi NT_s f)} e^{-j2\pi \frac{(N-1)}{2} T_s f} \tag{3.106}$$

while the F.T. for the discrete window in (3.105) is given by

$$W_d(f) = \frac{\sin(\pi N T_s f)}{\sin(\pi T_s f)} e^{-j2\pi \frac{(N-1)}{2} T_s f}. \tag{3.107}$$

An important and useful equivalence can be used to obtain (3.107) from a summation of analog spectra like (3.106). This equivalence is in general expressed as follows:

$$\boxed{W_d(f) = \frac{1}{T_s} \sum_{m=-\infty}^{+\infty} W_a(f - m f_s)} \tag{3.108}$$

which is an expression of the sampling theorem for this specific case. Then, by using the definition of normalized frequency, $f_n = \frac{f}{f_s} = T_s f$, the relation in (3.108) can be rewritten as

$$W_d(f) = N \sum_{m=-\infty}^{+\infty} \frac{\sin(\pi N (f_n - m))}{\pi N (f_n - m)} e^{-j2\pi \frac{(N-1)}{2}(f_n - m)} \tag{3.109}$$

then, from (3.107) and (3.109), we have that

$$\frac{\sin(\pi N f_n)}{\sin(\pi f_n)} = N \sum_{m=-\infty}^{+\infty} \frac{\sin(\pi N (f_n - m))}{\pi N (f_n - m)} e^{j\pi (N-1) m}. \tag{3.110}$$

This last relation is satisfied for any f_n and, after some simple manipulations, leads to the following corollary

$$\frac{1}{sin(\pi f_n)} = \frac{1}{\pi f_n} + \frac{2 f_n}{\pi} \sum_{m=1}^{\infty} \frac{(-1)^m}{(f_n^2 - m^2)} \tag{3.111}$$

which corresponds to a valid expansion for the cosecant for any real value of (πf_n).

3.B Appendix: DFT Properties and Fractional shift Synthesis

The DFT operation and its inverse are respectively defined by

$$\mathrm{DFT}(x[n]) = X[k] = \sum_{n=0}^{N-1} x[n] e^{-j2\pi \frac{k}{N} n}$$

$$\mathrm{DFT}^{-1}(X[k]) = x[n] = \frac{1}{N} \sum_{k=0}^{N-1} X[k] e^{j2\pi \frac{k}{N} n}$$

.

Let the DFT for a set of N samples of an unitary window be denoted by

$$U_N[k] \;=\; U_N\left(e^{j2\pi \frac{k}{N}}\right) = \widetilde{U}_N\left(\frac{k}{N}\right) = \mathrm{DFT}(1_N[n]). \tag{3.112}$$

Thus, with the shorthand notation $\widetilde{U}(\frac{k}{N})$ defined above, we have

$$\widetilde{U}_N\left(\frac{k}{N}\right) = \sum_{n=0}^{N-1} e^{-j2\pi \frac{k}{N} n} = \frac{\sin(\pi k)}{\sin(\pi k/N)} e^{-j\pi k \frac{N-1}{N}}. \tag{3.113}$$

The DFT is, in general, related with the FT of the discrete signal $x[n]$ as follows:

$$X(e^{j2\pi f_n}) = \frac{1}{N} \sum_{k=0}^{N-1} X[k] U_N\left(e^{j2\pi (f_n - \frac{k}{N})}\right) \tag{3.114}$$

where the N DFT values are used as interpolation coefficients in combination with a set of shifted base functions for interpolation which are, in this case, given by the discrete sincs $U_N(\cdot)$.

Thus, using (3.114), we can verify that

$$\begin{aligned} \widetilde{U}_N\left(\frac{p-r}{N}\right) &= \frac{1}{N} \sum_{k=0}^{N-1} \underbrace{U_N[k]}_{\widetilde{U}_N\left(\frac{k}{N}\right)} \widetilde{U}_N\left(\frac{p-r}{N} - \frac{k}{N}\right) \\ &= \frac{1}{N} \sum_{k=0}^{N-1} \widetilde{U}_N\left(\frac{k}{N}\right) \widetilde{U}_N\left(\frac{(p-k)-r}{N}\right) \end{aligned} \tag{3.115}$$

and, introducing the change of variable $p - k = m$, we have

$$= \frac{1}{N} \sum_{m=p-N+1}^{p} \widetilde{U}_N \left(\frac{p-m}{N} \right) \widetilde{U}_N \left(\frac{m-r}{N} \right)$$

and since $\widetilde{U}_N \left(\frac{\cdot}{N} \right)$ is periodic over N, we change the limits of the summation remaining over one period. This gives

$$= \sum_{m=0}^{N-1} \underbrace{\left[\frac{1}{N} \widetilde{U}_N \left(\frac{m-r}{N} \right) \right]}_{\alpha_r(m)} \widetilde{U}_N \left(\frac{p-m}{N} \right) \tag{3.116}$$

which is finally expressed as the equality

$$\widetilde{U}_N \left(\frac{p-r}{N} \right) = \sum_{m=0}^{N-1} \alpha_r(m) \widetilde{U}_N \left(\frac{p-m}{N} \right). \tag{3.117}$$

Since no restrictions were assumed for r, it may be any fractional value in the range $[0, 1]$, while $0 \leq m \leq N-1$ is an integer. Thence, it is possible to sinthetize any fractional delay using a combination of integer indexed delays over the same FT.

Now, using (3.113) and recalling that for synchronous reception the discrete window $w_T[n]$ starts at $T_{CE} - \frac{T_s}{2}$, which is equivalent to the sample time N_{CE}, we have

$$\begin{aligned} \widetilde{W}_T(f_n) &= \sum_{n=-\infty}^{+\infty} w_T[n] e^{-j2\pi f_n n} = \sum_{n=N_{CE}}^{N+N_{CE}-1} e^{-j2\pi f_n n} \\ &= \frac{\sin(\pi N f_n)}{\sin(\pi f_n)} e^{-j2\pi f_n (N_{CE} + \frac{N-1}{2})} \\ &= \widetilde{U}_N(f_n) e^{-j2\pi f_n N_{CE}}. \end{aligned} \tag{3.118}$$

Hence,

$$\widetilde{U}_N(f_n) = \widetilde{W}_T(f_n) e^{j2\pi f_n N_{CE}}. \tag{3.119}$$

The equality in (3.117) is expressed as

$$\widetilde{W}_T \left(\frac{p-r}{N} \right) e^{j2\pi N_{CE} \frac{p-r}{N}} = \sum_{m=0}^{N-1} \alpha_r(m) e^{j2\pi N_{CE} \frac{p-m}{N}} \widetilde{W}_T \left(\frac{p-m}{N} \right) \tag{3.120}$$

and

$$\widetilde{W}_T \left(\frac{p-r}{N} \right) = \sum_{m=0}^{N-1} \underbrace{\alpha_r(m) e^{j2\pi N_{CE} \frac{r-m}{N}}}_{\beta_r(m)} \widetilde{W}_T \left(\frac{p-m}{N} \right) \tag{3.121}$$

wherein

$$\begin{aligned}\beta_r(m) &= \alpha_r(m)e^{j2\pi N_{CE}\frac{r-m}{N}} \\ &= \frac{1}{N}\widetilde{U}_N\left(\frac{m-r}{N}\right)e^{j2\pi N_{CE}\frac{r-m}{N}}\end{aligned} \tag{3.122}$$

obtained using the $\alpha_r(m)$ previously defined in (3.116). Then, we use the relation in (3.119) obtaining

$$\beta_r(m) = \frac{1}{N}\widetilde{W}_T\left(\frac{m-r}{N}\right). \tag{3.123}$$

and therefrom, for the fractional index $r = \frac{T}{T_2}m_2' = \frac{N}{N_2}m_2'$, we have the final expression for $\beta_r(m)$:

$$\boxed{\beta_{\frac{T}{T_2}m_2'}(m) = \frac{1}{N}\widetilde{W}_T\left(\frac{m}{N} - \frac{m_2'}{N_2}\right)} \tag{3.124}$$

3.C Appendix: Diagonality of S

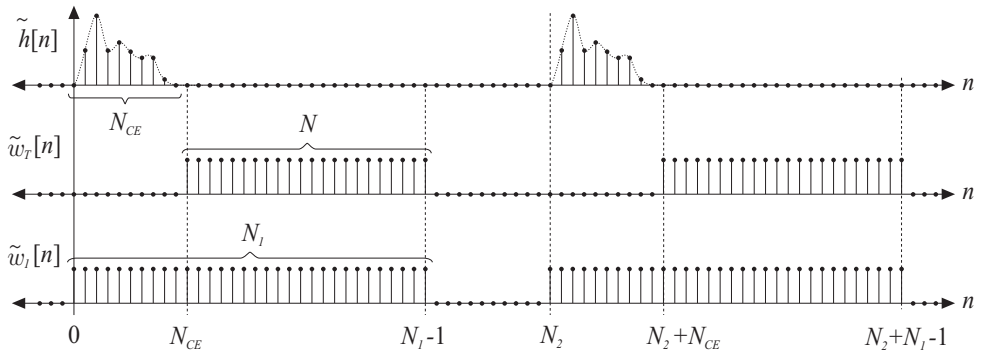

Figure 3.23:

In section 3.4, the matrix $\mathbf{S}$ was obtained to define the transference of an N-length vector $\mathbf{b}_x$ containing the input M-QAM symbols, to the final output $\mathbf{b}_y$ according to:

$$\mathbf{b}_y = \mathbf{S}\mathbf{d}_x = \sum_{m'=0}^{N-1} d_{m'}\mathbf{s}_{m'} \tag{3.125}$$

We have the elements of this $(N \times N)$ square matrix defined in general by:

$$\boxed{[\mathbf{S}]_{q,m'} = \frac{T_s}{N \cdot N_2} \sum_{m_2'=0}^{N_2-1} \widetilde{H}\left(\frac{m_2'}{N_2}\right) \widetilde{W}_T\left(\frac{q}{N} - \frac{m_2'}{N_2}\right) \widetilde{W}_1\left(\frac{m_2'}{N_2} - \frac{m'}{N}\right)} \tag{3.126}$$

where $\widetilde{H}(f_n)$, $\widetilde{W}_T(f_n)$ and $\widetilde{W}_1(f_n)$ are discrete FTs of the sequences $h[n]$, $w_T[n]$ and $w_1[n]$ respectively . All these sequences are of duration N_2 and the discrete time relations between them are shown in figure 3.23 for their respective periodic extensions with period N_2. Here the window $w_T(t)$ is defined synchronous starting at T_{CE} for notation simplicity.

We are now interested in determining the structure of $\mathbf{S}$, in particular we expect to demonstrate that it is a diagonal matrix, to find the expression for the elements of diag$\{\mathbf{S}\}$. Let us first consider that

$$w_T[n] \overset{FT}{\longleftrightarrow} \widetilde{W}_T(f_n) \tag{3.127}$$

$$w_T^*[n] \overset{FT}{\longleftrightarrow} \widetilde{W}_T^*(-f_n) \tag{3.128}$$

and, since for this real sequence $w_T^*[n] = w_T[n]$, we can rewrite the first expression as

$$[\mathbf{S}]_{q,m'} = \frac{T_s}{N \cdot N_2} \sum_{m_2'=0}^{N_2-1} \widetilde{H}\left(\frac{m_2'}{N_2}\right) \widetilde{W}_T^*\left(\frac{m_2'}{N_2} - \frac{q}{N}\right) \widetilde{W}_1\left(\frac{m_2'}{N_2} - \frac{m'}{N}\right). \tag{3.129}$$

In this expression, the summation index m_2' determines that the continuous and periodic FTs are sampled within one period each. This allow us to use the associated DFT values instead of the continuous expressions. For this purpose, the modulation property of the DFT, usually presented for integer shifts, can be extended for a general non-integer shift k_0 in the following form:

$$x[n]e^{j2\pi k_0 n} \overset{DFT}{\longleftrightarrow} X[k - k_0 N]$$

with

$$X[k - k_0 N] = X[k] \circledast \frac{\sin\left(N\pi(\frac{k}{N} - k_0)\right)}{\sin\left(\pi(\frac{k}{N} - k_0)\right)} e^{-j\pi\left(\frac{k}{N} - k_0\right)(N-1)}.$$

Here, $X[k]$ is the DFT of a sequence $x[n]$ with lenght N and the non-integer shift k_0 is obtained as the interpolation of the DFT values using sinc functions. Then, considering the periodic extensions of the three sequences and using the definition of the IDFT, we apply the DFT modulation properties to derive from (3.129) a useful expression given by

$$\begin{aligned} \widetilde{z}[n] &= \widetilde{h}[n] \circledast \left(\widetilde{w}_T[n]e^{j2\pi\frac{q}{N}n} \circledast \widetilde{w}_1[n]e^{j2\pi\frac{m'}{N}n}\right) && (3.130) \\ &= \frac{1}{N_2} \sum_{m_2'=0}^{N_2-1} H[m_2'] W_T\left[m_2' - \frac{q}{N}N_2\right] W_1\left[m_2' - \frac{m'}{N}N_2\right] e^{j2\pi\frac{m_2'}{N_2}n} && (3.131) \end{aligned}$$

where evaluating

$$\frac{T_s}{N}\widetilde{z}[0] \tag{3.132}$$

results in an equivalent expression for (3.129). Thence, developing the convolution at the right hand side of (3.130), we observe

$$\begin{aligned} \widetilde{z}[n] &= \widetilde{h}[n] \circledast \left(\widetilde{w}_T[n]e^{j2\pi\frac{q}{N}n} \circledast \widetilde{w}_1[n]e^{j2\pi\frac{m'}{N}n}\right) \\ &= \widetilde{h}[n] \circledast \left[\sum_{\ell=0}^{N_2-1} w_T[\ell]e^{j2\pi\frac{q}{N}\ell}\widetilde{w}_1[n-\ell]e^{j2\pi\frac{m'}{N}[n-\ell]}\right] \\ &= \widetilde{h}[n] \circledast \left[\sum_{\ell=0}^{N_2-1} w_T[\ell]\widetilde{w}_1[n-\ell]e^{j2\pi\left[\frac{m'}{N}n + \frac{q-m'}{N}\ell\right]}\right] \\ &= \sum_{p=0}^{N_2-1} \widetilde{h}[p] \sum_{\ell=0}^{N_2-1} w_T[\ell]\widetilde{w}_1[n-p-\ell]e^{j2\pi\left[\frac{m'}{N}(n-p) + \frac{q-m'}{N}\ell\right]} && (3.133) \end{aligned}$$

and now, evaluating for $n = 0$,

$$\begin{aligned}\widetilde{z}[0] &= \sum_{p=0}^{N_2-1} \widetilde{h}[p] \sum_{\ell=0}^{N_2-1} w_T[\ell]\widetilde{w}_1[-p-\ell]e^{j2\pi\left[\frac{(q-m')\ell-m'p}{N}\right]} \\ &= \sum_{p=0}^{N_{CE}-1} \widetilde{h}[p] \sum_{\ell=N_{CE}}^{N_1-1} \widetilde{w}_1[-p-\ell]e^{j2\pi\left[\frac{(q-m')\ell-m'p}{N}\right]} \end{aligned} \tag{3.134}$$

where the limits of the inner summation have been restricted to consider only the $N = N_1 - N_{CE}$ non-zero elements of $w_T[\ell]$ (see figure where $\widetilde{w}_T[n] = 1$ for $N_{CE} + kN_2 \leq n \leq N_1 + kN_2 - 1$). Similarly, the limits of the outer summation have been limited to $[0, N_{CE}]$ according to the finite time response defined for $h[n]$.

Then, in (3.134) it is easy to observe that

$$z[0] = 0 \ ; \text{ for } m' \neq q \ , \ (m', q) = \{1, 2, 3, \ldots, N\}$$

whence we deduce that $\mathbf{S}$ is a diagonal matrix. Now, for $m' = q$, the expression(3.134) becomes

$$\widetilde{z}[0] \mid_{m'=q} = \sum_{p=0}^{N_{CE}-1} \widetilde{h}[p]e^{-j2\pi\frac{m'}{N}p} \sum_{\ell=N_{CE}}^{N_1-1} \widetilde{w}_1[-p-\ell] \tag{3.135}$$

and, since $\sum_{\ell=N_{CE}}^{N_1-1} \widetilde{w}_1[-p-\ell] = N$ for $0 \leq p \leq N_{CE} - 1$, this is reduced to

$$\widetilde{z}[0] \mid_{m'=q} = N \sum_{p=0}^{N_{CE}-1} \widetilde{h}[p]e^{-j2\pi\frac{m'}{N}p}. \tag{3.136}$$

Finally, since $h[p] = 0$ for $N_{CE} \leq p \leq N_2 - 1$, we can extend the upper limit of this last summation to $N-1$ in order to evaluate the DFT of the zero padded set $[\mathbf{h}\ \mathbf{0}]^T$ with length N. Thus, (3.136) is rewritten as

$$\widetilde{z}[0] \mid_{m'=q} = N \sum_{p=0}^{N-1} \widetilde{h}[p]e^{-j2\pi\frac{p}{N}m'} = NH[m']. \tag{3.137}$$

Hence, using (3.137) to evaluate (3.132), the elements of the main diagonal of $\mathbf{S}$ are given by

$$[\mathbf{S}]_{m'=q} = \frac{T_s}{N}\widetilde{z}[0] \mid_{m'=q} = T_s H[m'] \tag{3.138}$$

This is, the N elements at the main diagonal of $\mathbf{S}$ correspond to the DFT values of the periodic extension (with period N) of the time-limited impulse response $h[n]$ given by

$$\widetilde{h}_N[n] = h[n] * \sum_{m=-\infty}^{+\infty} \delta[n + Nm]$$